LBL-13393

Lawrence Berkeley Laboratory

UNIVERSITY OF CALIFORNIA

RECEIVED
LAWRENCE
BERKELEY LABORATORY

FEB 22 1982

LIBRARY AND
DOCUMENTS SECTION

Materials & Molecular Research Division

TWO-BODY, DRY ABRASIVE WEAR OF Fe/Cr/C EXPERIMENTAL ALLOYS --- RELATIONSHIP BETWEEN MICROSTRUCTURE AND MECHANICAL PROPERTIES

Chi Kong Simon Kwok
(M.S. thesis)

January 1982

TWO-WEEK LOAN COPY

This is a Library Circulating Copy which may be borrowed for two weeks. For a personal retention copy, call Tech. Info. Division, Ext. 6782

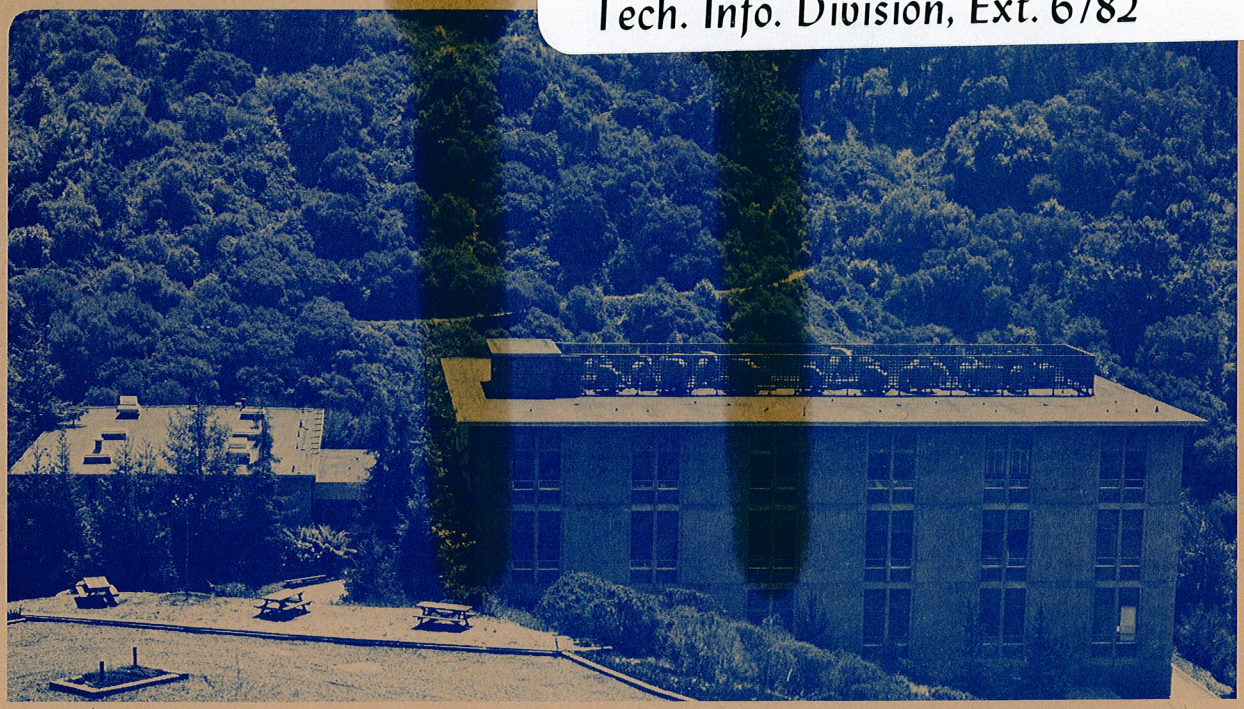

Prepared for the U.S. Department of Energy under Contract W-7405-ENG-48

LBL-13393 c.2

TWO-BODY, DRY ABRASIVE WEAR OF Fe/Cr/C EXPERIMENTAL ALLOYS --- RELATIONSHIP BETWEEN MICROSTRUCTURE AND MECHANICAL PROPERTIES

Chi Kong Simon Kwok

Materials and Molecular Research Division
Lawrence Berkeley Laboratory
and
Department of Materials Science and Mineral Engineering
University of California
Berkeley, California 94720

ABSTRACT

A systematic study of abrasive wear resistance of Fe/Cr/Mn based alloys has been carried out using a two body pin-on-disc wear machine. Abrasives used were silicon carbide, alumina and quartz.

The objective of this study was to evaluate the abrasive wear resistance and to investigate the relationships between microstructure, mechanical properties, and abrasive wear resistance for these experimental alloys. Several commercial alloys were also tested to provide a basis for comparison.

The goal of this study was to develop information so as to improve wear resistance of these experimental alloys by means of thermal treatments. Grain-refinement by double heat treatment was carried out in this research.

Results showed that bulk hardness and tensile strength are both very important factors in abrasive wear. The experimental alloy, which has superior tensile and toughness properties, has a better wear resistance than most of the commercial alloys tested. Grain-refinement by double heat treatment improved the toughness but appeared to have little effect on the abrasive wear resistance.

This manuscript was printed from originals provided by the author.

I. INTRODUCTION

Wear is a form of mechanical failure that is very general but poorly understood. Maintenance and replacement of worn machinery represents a significant cost to industry. More often, the waste of time and manpower to replace the worn parts and the loss due to the shutdown greatly exceed the actual cost of the replaced parts. In the United States alone, an estimated $16 billion per year can be saved if the proper wear prevention is implemented[1].

Among various wear mechanisms, such as erosion, sliding wear and others, it is abrasive wear which is most frequently encountered. Abrasion is commonly found in earth-moving, mining, argiculture and other industries. In recent years, there has been an urgent need to decrease the dependence on crude oil due to its escalating cost and unstable supply. A lot of interest has been generated in the substitution of crude oil by other energy sources. Coal, which is abundant in the United States, has now become a more promising and viable alternative. The increase in coal mining and processing activities demands a new class of alloy which is inexpensive, tough and wear-resistant. Toughness, as well as abrasive wear resistance is equally important since many processing operations involve continuous impact and wear. Failure can occur either when the part breaks through impact or is worn to a point where it can no longer function properly.

In recent years a program[2-10] has been systematically carried out at Berkeley to investigate the effect of alloying elements and heat treatment on the martensitic microstructure of a group of ternary Fe/Cr/C and quaternary Fe/Cr/Mn/C alloys.

These experimental alloys have superior tensile strength and toughness as compared to many commercial alloys. In addition, a recent study[11] has also shown that their sliding wear resistance is greater than many commercial wear-resistant alloys. Since the majority of wear problems arising in the mining industries involve two body and three body abrasion, it is important therefore to understand the abrasive wear characteristics of these steels and their responses to thermal treatments.

Wear is defined as the removal or displacement of material by surface interaction. The main difference between abrasive wear and other modes of wear such as sliding wear, corrosive wear, etc. is the presence of hard, angular abrasives during wear[12]. Although it is possible to abrade using abrasives of relative hardness (hardness of abrasive/hardness of base material) less than one[13], abrasion only becomes effective when relative hardness is greater than 1.2[46]. However, the cutting efficiency of the abrasive does not depend solely on the hardness of the abrasive. The grit size, angularity (rake angle) and bond strength (adherence to the matrix) are all important. Using a single diamond scratch experiment, Murray et al.[14] found that machining can only occur at a certain range of rake angles, depending on the hardness of the base alloy. A simplified mechanism of abrasive wear has been proposed by Rabinowicz[15] in which grooves are cut with the abrasive forming continuous chips. The assumptions are (i) the wear loss is equal to the total volume of grooves formed and, (ii) all contacting points are effective in cutting. However, the wear rate derived from this mechanism is much higher than actually observed in experiments. Severe plastic deformationalso occurs and forms ridges besides the grooves; these ridges contribute very little to wear loss.

Delamination[16-18] can occur at these ridges by nucleation or subsurface cracks and their subsequent joining by shear deformation of the surface (see Figure 18). This proposed theory predicted the presence of plate-like wear particles and large plastic deformation of the surface layer.

II. EXPERIMENTAL PROCEDURES

A. Alloy Preparation and Heat Treatment

(1) Experimental alloys. The composition of the experimental alloys (designated Quatough steels) and commercial alloys are listed in Table 1. The Quatough alloys, designed for high strength and toughness[19] were melted by Daido Steel Co., Japan. The vacuum-induction melts were cast into 20 lb. ingots and subsequently forged to 1 inch thick and 2.5 inch wide slabs. Then, they were homogenized at 1200°C for 24 hours and furnace cooled.

Three different heat treatments were applied to the experimental alloys, namely HT(I), (II) and (III) as shown diagrammatically in Fig. 1. Their relative merits will be discussed in a later section. Basically, the heat treatment involved high temperature austenitizing (1100°C), oil quenching and subsequent tempering. HT(III) and HT(II) require a second low temperature austenitizing (870°C) and subsequent quenching and tempering with or without an intermediate 200°C tempering, respectively. All the austenitizing treatments were carried our in a vertical tube furnance under an inert gas atmosphere. At the end of the austenitization, specimens were quenched into agitated oil. All tempering treatments (200°C to 500°C) were performed by immersing the specimens into a salt pot for one hour and then quenching into cold water.

(2) Commercial alloys. All commercial alloys, Abrasaloy, Astralloy and Firmex were used in as-received conditions. AISI 1020 was purchased and used in a hot-rolled condition.

B. Metallography

(1) Optical metallography. Specimens for optical metallography

were cut from heat-treated material, mounted in cold mount resin, abraded on silicon carbide paper down to 600 grit, and then polished with 1μm diamond paste on a microcloth. A 5% nital etchant was used to reveal the microstructures.

(2) Scanning electron microscopy and energy dispersive analysis of X-ray. Scanning electron microscopic studies were carried out on the worn surface of the specimens using an AMR-1000 scanning electron microscope operated at 20kV. An energy dispersive X-ray analyser (EDAX) attached to the microscope was used to identify the different constituents present on the worn surfaces, and on the debris.

(3) Transmission electron microscopy. Thin foils of ∿500μm thickness were cut from the heat-treated alloys via a Diamet saw. These slices were then chemically thinned to 125μm in a 4% solution of HF in H_2O_2. 3.0mm discs were obtained by spark cutting and were abraded down to 25-50μm thickness by 400/600 grit abrasive paper. Final polishing was achieved using a twin-jet electropolisher at room temperature, with a solution of 75g of CrO_3. 400ml Ch_3COOH and 21ml distilled water. The polishing voltage was 40-45 volts at 50-55 milliamps. Once suitable thin foils were produced, transmission electron microscopy was carried out, using either a JEM7A or a Philips 301 electron microscope, both operating a 100kV.

C. Wear Properties

(1) Wear specimen preparation. Wear pins were cut from the heat-treated specimens in the form of rectangular bars. Then they were machined to 6.35mm in diameter by 20mm long hemispherically tipped cylindrical pins as shown in Figure 2. The tips were ground to exact

size under flood cooling to prevent any heat-induced microstructural change.

The specimens were hand-cleaned in N-heptane to remove oil and dirt, and then ultrasonically cleaned by ethyl alcohol for 5 minutes before finally being placed in a vacuum desiccator to remove any moisture left on the surface.

The specimens were weighed prior to each wear test on a Mettler H54AR analytical balance to an accuracy of + 0.01mg. Three measurements were taken for each pin and the median value recorded. After every wear test, the wear pins were carefully dusted off by a gentle stream of compressed helium gas and reweighed. The weight loss was then determined and converted to wear resistance as shown below:

$$\text{Wear resistance} = 1/\text{wear rate}$$

$$= \frac{\text{length of wear path}}{\text{volume of material removed}}$$

$$= \frac{(\text{material density})\ (\text{length of wear path})}{\text{weight loss}}\ \text{mm/mm}^3$$

(2) Wear test. The two-body, dry abrasive wear tests were performed on a pin-on-disc wear machine which simulated high stress abrasion. The wear pins were worn against abrasive paper for 10 revolutions at a rotational speed of 20 rpm under 1 kg deadweight load. A spiral wear track, about 2.2 meters in length, was generated as the wear pin moved transversely across the abrasives. A spiral path was used to ensure that unworn abrasives were encountered on each revolution. The worn specimens were lifted off automatically by a mechanical relay after 10 revolutions.

A break-in run was carried out prior to each of the three wear tests performed on each pin. The subsequent weight losses were measured and a

mean value was calculated. Two pins were tested for each material, using the same experimental conditions. Finally, the two mean values for weight loss were combined and converted to a value of wear resistance, to generate one datum point. The experimental data were found to be quite reproducible giving only a 3-5% scatter band.

Three abrasives, 120 grit SiC, 120 grit carborundum Al_2O_3, and 40 grit flint SiO_2 were used in the wear test to assess the effect of abrasive geometry and hardness on abrasive wear.

III. RESULTS

A. Optical Metallography

Optical metallography was performed to confirm the microstructure and prior austenite grain size of the experimental material used in the wear tests. The experimental alloys were found to be composed of uniform packets of lath matensite, with no dissolved carbides observed. This agreed with previous work[20]. Double heat-treatments (II) and (III) decreased the grain size by an order of magnitude (from 270 to 30 microns) in comparison to the conventional heat treatment (I), (see Figure 3).

The commercial wear-resistant alloys Abrasaloy, Astralloy and Firmex all had a martensitic and/or bainitic microstructure. In addition, elongated MnS inclusions were observed in the Firmex alloy (see Figs. 4(a), (b), (c)). The AISI 1020 alloy was found to have a pearlitic/ferritic microstructure, an example of which is shown in Fig. 4(d).

B. Transmission Electron Microscopy

(1) Experimental alloys. In recent years the TEM microstructures of Fe/3Cr/2Mn/0.5Mo/.3C have been well-documented[20]. TEM was carried out to confirm these observations and the results agree with previous studies showing that the as-quenched microstructure was highly-dislocated lath martensite with continuous interlath film or retained austenite. The typical lath dimensions were found to be 0.5 microns in width and 5-10 microns in length (Figure 5).

Upon 200°C tempering, $\langle 110 \rangle_\alpha$ Widmanstatten cementite precipitates were observed within the martensite laths and were typically 0.3 - 0.5μm long and 200Å to 500Å wide. At 300°C tempering, cementite precipitation was observed both inside the lath and at the lath boundaries (Figure 6).

At 400°C and 500°C tempering, extensive carbide precipitation inside the laths, and discontinuous stringers of carbide at lath boundaries were observed. Spheroidization appeared to have started at 400°C and continued at 500°C tempering.

TEM studies on double heat-treated specimens showed a similar transformation with tempered martensite embrittlement beginning at 300°C. The martensite packet size was smaller in comparison to conventional heat-treated specimen, but the lath width was relatively unchanged.

(2) Commercial alloys. Interlath and intralath carbides were observed in Abrasaloy, a consequence of the bainitic structure. Astralloy, however, appeared to have a complex martensitic microstructure with a small amount of microtwins present, whereas Firmex was found to have a non-uniform bainitic/martensitic microstructure in which extensive carbide precipitation was observed[11].

Although the above commercial alloys had microstructures similar to those observed in the experimental alloys, there were important differences that resulted in the greater toughness of the latter viz. the uniformity of martensite packets and the presence of continuous interlath films of retained austenite.

(C) Mechanical properties. A summary of the mechanical properties of the experimental alloys is shown in Table 2 and Fig. 7[20]. The ultimate tensile strength, yield strength, Charpy toughness and hardness all show a similar tempering response in that they all increase slightly from the as-quenched condition at 200°C tempering, then decrease drastically after 300°C, and continue to decrease drastically at 400°C and 500°C tempering. This abrupt decrease in mechanical properties is mainly due to tempered

martensite embrittlement (TME), caused by the transformation of interlath austenite to deleterious interlath carbide stringers at temperatures greater than 300°C[45].

Some of the mechanical properties of the commercial alloys were provided by their respective manufacturers (see Table 2).

D. Wear test. Wear tests were performed on a 2-body pin-on-disc wear machine, and a summary of the wear data is shown in Table 3.

The main advantages in using the pin-on-disc type test are in its ease of parameter control and good reproducibility. It is, however, different from most tribological environments encountered in commercial wear situations. Nonetheless, similar trends exist when pin-on-disc laboratory tests were compared to field tests[21,22].

Three abrasives were used in the tests and their cutting efficiency in wear can be ranked in the following order starting with the most efficient: Al_2O_3, SiC and SiO_2. Even though SiC is harder than Al_2O_3, the wear rate was lower mainly because Al_2O_3 had a better bond-adherence between the abrasives and the supporting media (Figure 13).

The wear resistance of vacuum-melted Fe/3Cr/2Mn/.5Mo/.3C steel was found to be superior to Firmex, Abrasaloy, Astralloy and AISI 1020 and generally was 20-40% higher than these commercial alloys. The wear resistance was also measured as a function of tempering temperature for the experimental alloys and compared to the equivalent plots for impact toughness, tensile strength, yield strength and hardness (see Figs. 7 and 8). The effect of tempering temperature on the wear resistance is effectively the same for the as-quenched and the 200°C tempered state. However, the wear resistance dropped abruptly after tempering at 300°C,

only to gradually increase again (by a total of 5%) after 400°C and 500°C tempering.

When SiC was used in the wear tests, there was little difference in wear resistance between the double heat-treated and the conventional single heat-treated specimens. However, when quartz (SiO_2) was used, there was some (see Table 3) measureable improvement observed in the grain-refined specimen. When the commercial alloys were tested with each of the three different abrasives, Abrasaloy, Firmex and Astralloy all had similar wear rates. As Astralloy had a higher ultimate tensile strength (UTS) and hardness than Firmex and Abrasalloy, it is interesting to note that Astralloy did not have a better wear resistance than the other two commercial alloys.

E. Scanning electron microscopy. The general wear surface produced by abrasive wear is comprised primarily of micro-machining grooves covering the entire worn surface. The grooves were produced by abrasive particles penetrating the surface and shearing off material. Severe lateral flow of material occurred in the direction of abrasion.

There seemed to be no difference in the surface appearance of a given steel when worn by either SiC or Al_2O_3. However, when SiO_2 was used, more plastic flow was observed than with the other two abrasives (Figure 16). The "apparent" groove width was 20-100μm, but because overlapping of the wear tracks occurred (produced by repeated abrasion), it was not possible to determine a more accurate measurement. The material with the harder surface appeared to have well-defined wear tracks, but for materials with lower surface hardness, more plastic, multidirectional flow occurred.

Energy dispersive X-ray spectroscopy (EDAX) was used to show the presence of a few small pieces of fractured abrasive particles embedded on the wear surface. This indicated high stress abrasion[23] which is commonly defined as the abrasive wear which occurs when the fracture stress of the abrasive particle is exceeded.

Three types of abrasives; SiC, Al_2O_3, and SiO_2 were used in the wear tests and comparsions of their appearance before and after wear tests are shown in Figure 13. For all three abrasives, only small portion of all the sharp cutting tips were fractured during the wear test which indicated that only small percentages of abrasive particles exceeded their load-bearing capacity and the remaining particles are still effective for further abrasion. The average diameter of a silicon carbide is about 80 μm. The average groove width of Quatough steel worn by SiC is around 20 - 40 μm (see Figure15). These approximate measurements agree with each other and implied that only part of the abrasive tip is involved in micromachining. The depth of wear grooves is a function of surface stress state, material properties and abrasive geometry.

Among all the wear surface shown in Figure14, Quatough steel tempered at 200C, which has the highest wear resistance in this test group, has the fewest wear scars than the other alloys. The appearances of the wear surfaces of Quatough alloy tempered at 500C, Abrasaloy, Astrolly and Firmex are verysimiliar while the wear surface of AISI 1020 has the highest degree of roughness indicated more ploughing and deeper groove-cutting. As the hardness of a material increases, more abrasive particles have rake angles that are greater than critical rake

angle and thus there is an increase in number of particles available for micromachining, or less ploughing occurs.

Figure 15 shows the general wear surface at a high magnification. Long, well-defined wear grooves were found running in the direction of abrasion. Ridges formed alongside the edge of grooves are due to severe plastic deformation. Also, fractured abrasive particles embedded in the base alloy are frequently observed.

Figure 16(b) shows an area where the microcutting was impeded by hard particle and the abrasive particle broke off from its supporting media. A wedge of alloy (area A) and a metal chip (area B) were partially sheared and appeared to be lifted off by residual tensile stress. Small abrasive particles were entrapped in the cavity (area C) and are identified by the silicon peak in the EDAX picture (see Figure 15(d)).

X-ray mappings on iron and silicon were used to identify the 1020 wear debris from the SiC abrasives. (see Figure 16). Size of debris varies from 5-40 μm in diameter and take all from one shape. Some debris appear to be plate-like and might be formed by delamination.

Micrographs from Figure 17 were taken with Quatough alloy tempered at 500C, area B in Figure 17(a), is an evidence of 2 subsurface cracks propagate and join. This particle B may be lifted up by residual tensile stress produced by the passing of abrasives and will have the same appearance as in A after breaking off from the matrix, even though this wear mechanism is not dominated in the wear test, it shows that delamination can take place in abrasive wear.

IV. DISCUSSION

(1) Effect of mechanical properties on abrasive wear. Hardness, tensile strength and ductility strongly affect abrasive wear resistance. Hardness is very important in determining abrasive wear resistance because it controls the depth of penetration by the abrasives. Therefore, it is not surprising to find that the wear resistance is directly proportional to the bulk hardness of many pure annealed[28-30] metals. For heat-treated steels, however, the slope of wear resistance versus hardness is found to be lower than that of pure metals[28]. Further study by Larsen-Basse[25] has confirmed this deviation, which can be explained by the decrease of the work hardening coefficient with an increase in hardness. Results from the present wear tests, as shown in Fig. 10, show a positive trend between hardness and wear resistance.

Ductility and hardness, determine the mode of wear--plowing or machining. Alloys with high ductility and low hardness, such as AISI 1020, are worn by extensive plowing in addition to micromachining. Whereas in the case of alloys with low ductility and high hardness, micromachining becomes the dominant mode of wear. Comparing the wear surfaces shown in AISI 1020 (low hardness and high ductility) has a small number of unidirectional grooves with highly plastically deformed scars, indicating extensive plowing as well as machining. Quatough steel, however, (high hardness with moderate ductility) has many well-defined grooves along the direction of wear indicating basic micromachining wear. The grooves present on the wear surface of 1020 appear to be deeper than those of the experimental steels and this may account for the higher wear rate of 1020 steel.

Abrasive wear resistance tends to increase with hardness[24-27], tensile strength and yield strength. Correlations of wearresistance and the above mechanical properties for a variety of ferrous alloys are shown in Figure 9, 10 and 12.

High yield strength resists plastic flow of material and increases the plastic work required before fracture occurs. During abrasive wear, a large amount of energy is consumed to surmount this plastic work before micromachining can occur. Hardness controls the depth of indentation of abrasive particle during abrasion and thus indirectly determines the wear groove depth. Since wear volume is directly proportional to the square of groove depth, increase surface hardness always improves the wear resistance.

An attempt to relate wear resistance with Charpy impact toughness yielded no apparent relationship as shown in Figure 11. No correlation is expected because the mechanism of a crack initiating at a prefabricated notch under an immense impact is entirely different from the cutting mechanism of abrasion.

(2) Effect of tempering on abrasive wear. There are three principal ways of strengthening the structure of steels: (a) alloying, (b) work hardening, and (c) heat treating.

(a) For most ferrous alloys, an increase in carbon content is the most effective way to increase wear resistance. Hardenability, bulk hardness and volume fraction of alloy and iron carbides, are all believed to be benefical to abrasive wear, resistance, and all increase with increasing carbon content. Previous studies[10,20] have shown that microstructural twinning occurs when the carbon content of experimental alloys is equal or greater

than 0.3%. Therefore, this posts an upper limit upon the carbon content of 0.3%, as twinned martensite is known to possess more inferior fracture and impact toughness properties than lath martensite. The addition of chromium to steel improves both strength and toughness and has a small but measurable effect in improving abrasive wear[31]. However, if 0.5% molybdenum is added and reducing Cr by 1% no detrimental effect upon either the high strength or the high toughness of the quaternary alloy occurs. Moreover, molybdenum may reduce the severity of temper embrittlement[32,33]. The final composition of Fe/3Cr/2Mn/0.5Mo/.3C gives optimum strength and wear properties without any sacrifice in toughness.

(b) Extensive work-hardening in the form of plowing always occurs during abrasive wear, so there is little profit in improving bulk hardness by cold work. The surface will work-harden regardless of prior cold work. Thus, the wear resistance is relatively independent of prior cold work[34,35].

(c) It is likely that improving the strength of the material through heat treatment will produce a corresponding increase in wear resistance. In the present experiment, Quatough steels have been subjected to different. tempering conditions (from as-quenched to 500°C tempering) after high tempering austenitization and oil quenching. Comparisons between wear resistance and hardness, tensile strength and yield strength show a similar trend (see Figs. 7 and 8). The wear resistance of the experimental alloys in the as-quenched state and 200°C tempered state are about equal but decrease abruptly at 300°C tempering. At 400°C and 500°C tempering, wear resistance is gradually increased by a total of 5%. The sharp decrease in both fracture toughness and wear resistance after 300°C

is a direct result of the onset of tempered martensite embrittlement. At this stage in tempering, the continuous films of interlath, retained austenite transform to iron carbides. It is likely that these carbides limit the plastic zone in front of any intralath crack to the width of the martensite lath, and thus promote unstable crack propagation.

At higher tempering temperatures, carbides continue to grow and eventually spherodize. A decrease in stress concentration at the tempered carbides due to spheroidization decreases the tendency of crack initiation at those Widmanstatten intralath carbides and easy crack-propagation through interlath carbides.

Ultimate strength, yield strength and hardness tempering curves all have a similar slope (up to 300°C tempering) to that of the wear resistance of the experimental alloy (Fig. 7). When the same material is considered with different mechanical properties due to different heat treating conditions, there is a possible direct proportionality between UTS, YS and hardness and its wear resistance. However, when different materials are compared (see Figs. 10 and 11), data points become more scattered. This occurs because wear rate is microstructurally sensitive so different microstructures (e.g. martensitic, bainitic, pearlitic, or ferritic) respond differently during abrasive wear.

Although the microstructures of the commercial alloys and the experimental alloys appear to be somewhat similar (martensitic or martensitic/bainitic complex), the inferior wear properties of commercial steels, may be due to their nonuniform distribution of large carbides and/or interlath carbide formation[36].

The effect of retained austenite on abrasive wear has been shown

to be beneficial by many investigations[37-40]. The enhancement of wear resistance by the retained austenite may be due to (i) the transformation induced plasticity (TRIP) that can absorb energy for fracture and produce local compressive stresses that impede microcrack formation, (ii) the presence of the ductile austenite film between the martensite laths discouraging microcrack nucleation and propagation. Previous evidence[41] has shown that crack propagation through a retained austenite phase was significantly arrested; (iii) an increase in work-hardening coefficient through TRIP or (iv) retention of retained austenite at lath boundary preventing brittle lath boundary carbide formation. In the case of the Quatough steels, the amount of retained austenite is about 2% in the as-quenched condition, decreasing abruptly to zero percent at or above 300°C tempering temperature. Because the experimental error involved in detecting retained austenite by X-ray diffractometry is typically >0.5%, it is difficult to establish any quantitative correlation between the amount of retained austenite and the wear resistance.

Mössbauer spectroscopy has been performed on both the experimental and commercial alloys to determine the volume fraction of retained austenite quantitatively[42]. The amount of retained austenite in the following steels--Quatough, Abrasaloy, Firmex and Astralloy--is 3.5%, 0.3%, 5% and 1.5%, respectively[11]. Again no conclusive, quantitative relationship between the amount of retained austenite and abrasive wear resistance is possible. The data in Table 3 show that although the commercial alloys have a different volume fraction of retained austenite, their wear resistance is almost identical. Nevertheless, in the case of low carbon, structural steels, the distribution and morphology of retained austenite

(interlath, intralath, thin, continuous film vs. block) may be more important than the relative amount present.

(3) Effect of grain-refinement on abrasive wear. For most ferrous alloy systems, it is generally true that the flow stress is inversely proportional to the square root of grain diameter[43,44]. Any heat treatment that refines the grain should improve the strength. Since hardness and ultimate tensile strength are well known for their beneficial role in abrasive wear[12], grain-refinement is one possible way to improve abrasive wear resistance.

From the results shown in Tables 2 and 3, the wear resistance, hardness, UTS and YS of the Quatough steel is relatively constant whereas fracture toughness and impact toughness increase moderately when subjected to double heat-treatment. Neither the tensile properties nor the wear resistance obey the classical Hall-Petch inverse square root relationship. However, they are in agreement with each other. This apparent discrepancy, in which the prior austenite grain diameter decreases an order of magnitude with little corresponding change in both tensile properties and wear resistance, can possibly be explained by (i) the martensite lath size, which does not noticely change under HT(II) and HT(III), and is a more fundamental parameter controlling the mechanical properties, most microcracks initiate either at an inclusion or a cracked cementite particle within the martensite lath, and they tend to propagate through the laths along their longitudinal lath axis in a zig-zag fashion, as laths change orientation from one packet to another. The nominal lath length is 5-10 μm, so they are much smaller than prior austenite grain size, the lath boundaries become effective barrier of crack propagation, or (ii) the high dislocation density due to the rapid oil quench; the

movement of dislocation is limited to very short distance before impingment occurs. A prior austenite grain diameter of 30 μm with HT(III) is too large to be an effective dislocation barrier.

The main benefit of double heat treatment is improving factor toughness by a fine redistribution of the interlath iron carbides in the matrix, and also increase the amount of retained austenite slightly in the alloy.

V. CONCLUSION

1. The best abrasive wear resistance of Fe/3Cr/2Mn/.5Mo/.3C is obtained in the as-quenched condition. However, a 200°C tempering gives optimum tensile and fracture toughness properties without an appreciable decrease in the wear resistance.

2. The wear resistance decreases sharply after 300°C tempering and is likely due to the transformation of interlath retained austenite to carbides.

3. Highly dislocated lath martensite with continuous film of retained austenite appears to be a preferable microstructure than either a banitic/martensitic or a ferritic/pearlitic microstructure for good wear resistance.

4. Grain-refinement by double heat treatment improves the toughness but appears to have little effect on the abrasive wear resistance.

5. Correlation between mechanical properties and wear resistance shows positive trend between tensile strength, hardness and wear resistance.

VI. ACKNOWLEDGEMENTS

The author wishes to express his sincere gratitude to Professor Gareth Thomas for his continued support and guidance. Deep appreciation is extended to Dr. Judy Rayment and William Salesky for their help and valuable discussions.

The author also wishes to thank Profs. I. Finnie and J.W. Morris, Jr. for their appraisal of the manuscript.

Helpful discussion with Dr. Warren Garrison, Dr. John Kung, Mehmet Sarikaya, Lew Rabenberg and Alvin Nakagawa are gratefully acknowledged.

Thanks are also due to Kathleen Brusse for typing this manuscript.

Finally, the author is deeply indebted to his parents for making this work possible.

This work was supported by the Director, Office of Energy Research, Office of Basic Energy Sciences, Division of Materials Science of the U.S. Department of Energy under Contract No. W-7405-ENG-48.

REFERENCES

1. H. P. Jost: Mechanical Engineering 97, 26 (1975).
2. G. Thomas: Met. Trans. 2, 2373 (1972).
3. S.K. Das and G. Thomas: Trans. A. S. M. 62, 659 (1969).
4. D. H. Huang and G. Thomas: Met. Trans. 2, 1587 (1971).
5. M. Raghavan and G. Thomas: Met. Trans. 2, 3433 (1971).
6. I. Lin Cheng and G. Thomas: Met. Trans. 3, 503 (1972).
7. J. McMahon and G. Thomas: Proc. 3rd Internat. Conf. on Strength of Metals and Alloys, Inst. of Metals, London 1, 180 (1973).
8. R.A. Clark and G. Thomas: Met. Trans. 6A, 969 (1975).
9. B.V.N. Rao and G. Thomas: Mat. Sci. and Eng. 20, 198 (1975).
10. B.V.N. Rao: Ph.D. Thesis, University of California, Berkeley, February 1978, LBL #7361.
11. W.J. Salesky; M.S. Thesis, University of California, Berkeley, June 1980, LBL #10994.
12. M.A. Moore, Wear 27, 1 (1974).
13. R.C. Richardson: Wear 10, 291 (1967).
14. M.J. Murray, P.J. Mutton and J.D. Watson: Proc. of the Internat. Conf. on Wear of Materials ASME (1979), 257.
15. E. Rabinowicz: Friction of Wear of Materials, John Wiley and Sons, Inc., New York, 1965.
16. N.P. Suh: Wear 25, 111 (1973).
17. S. Jahanmir and N.P. Suh: Wear 44, 17 (1977).
18. J.R. Fleming and N.P. Suh: Wear 44, 39 (1977).
19. B.V.N. Rao and G. Thomas: Met. Trans. A11, 411 (1980).
20. M. Sarikaya: M.S. Thesis, University of California, Berkeley, June 1979, LBL #9260.

21. P.J. Moroz, Jr. and J.J. Lorenzetti, Wear of Materials 1981, 280.

22. D.E. Diesburg and F. Borik, Symposium on Materials for the Mining Industry 1974, 15.

23. H. Avery: Wear of Materials 1977, ASME.

24. M.M. Khruschov: Inst. of Mech. Eng.; Proc. Conf. on Lubrication and Wear, London, 665 (1957).

25. J. Larson-Basse: Trans. AIME 236, 146 (1966).

26. R.C. Richardson: Wear 11, 245 (1968).

27. A. Misra: Ph.D. Thesis, University of California, Berkeley, September 1979.

28. M.M. Khruschov and M.A. Babichev: Friction and Wear in Machinery 11, 5 (1956).

29. M.M. Khruschov: Inst. Mech. Engrs. Proc. Conf. Lubrication and Wear (1957), 655.

30. C. Rubenstein: Wear 8, 70 (1965).

31. R.A. Garriga, M.S. Thesis, University of California, Berkeley, August 1979.

32. J.R. Rellick and C.J. McMahon, Jr.: Met. Trans. 5, 2439 (1974).

33. S.K. Barrarji, C.J. McMahon, Jr. and H.C. Feng: Met. Trans. 9A, 237 (1978).

34. M.M. Khruschov and M.A. Babichev: Friction and Wear in Machinery 19, 1 (1965).

35. K.H.R. Wright: Tribology 2 (3), 152 (1969).

36. P.L. Hurrick, Wear 22 (3), 291 (1972).

37. M.S. Bhat, V.F. Zackay and E.R. Parker, Proc. of 3rd. Conf. on Material for Coal Conversion and Ultilization, October 1978.

38. N.J. Kar: Wear of Material 1981, p. 415.

39. K.H. Zurn Gahr: Metal Progress, September 1979, 46.

40. P.L. Hurrick: Wear 26, 285 (1973).

41. D. Webster: Trans. A.S.M. 61, 816 (1968).

42. B. Fultz, M.S. Thesis, University of California, Berkeley, June 1978, LBL #7671.

43. E.O. Hall: Proc. Phys. Soc. Series B 64, 747 (1951).

44. N.J. Petch, J. Iron Steel Inst. 174, 25 (1953).

45. G. Thomas: Met. Trans. 9A, 439 (1978).

46. Metal Handbook, 603 (1978).

TABLE 1

Steel Composition

	C	Cr	Mn	Ni	Mo	Co	Si	Ti	V	Fe
QUATOUGH	0.26	3.11	1.98	0.01	0.50	-	-	-	-	Bal.
ABRASALOY	0.35	0.45	0.87	0.58	0.14	-	0.20	-	-	Bal.
ASTRALLOY	0.29	1.67	1.07	3.68	0.37	0.08	0.42	0.007	0.01	Bal.
FIRMEX	0.26	0.30	1.94	0.73	0.24	-	0.57	0.06	-	Bal.
AISI 1020HR	0.20	-	0.45	-	-	-	-	-	-	Bal.

TABLE 2

Mechanical Properties

Alloy	Tempering (Temp.(°C)	UTS (MPa)	YS (MPa)	Total Elongation(%)	Charpy Toughness(J)	Fracture Toughness(MPa-m)$^{1/2}$	Hardness (Rc)
Fe/3Cr/2Mn/0.5Mo/ 0.3C HT(I)	AQ	1744	1379	6.25	39.0	88	48.5
	200	1772	1413	7.0	47.0	121.6	48
	300	1420	1220	8.0	30.5		45
	400	1379	1172	8.1	30.0		42
	500	1338	1145	7.0	27.0		40.5
HT(II)	200	1724	1320	11.6	51.5	127.2	48
HT(III)	200	1724	1338	12.0	57.0	130.0	47
FIRMEX		1365	1269	11.0	20.3		40
ABRASALOY		1241	1207	12.0			40
ASTRALLOY		1661	1082	12.0	42.0		45
AISI 1020HR		448	331	36.0	87.0		$110H_B$
AISI 4340		1999	1551	10.0	17.6	49.5	52

TABLE 3. Wear Properties

Alloy		Tempering Temp. (°C)	Weight Loss/ Pass(mg)	Wear Resistance*	Weight Loss/ Pass(mg)	Resistance*	Weight Loss/ Pass(mg)	Resistance*
			120 grit SiC		40 grit SiO_2		120 grit Al_2O_3	
1) Fe/3Cr/2Mn/0.5Mo/0.3C	HT(I)	AQ	1.95	8879	1.61	10754	2.00	8657
2)		200	2.00	8657	1.66	10430	2.21	7843
3)		300	2.38	7275	1.87	9259	2.65	6534
4)		400	2.35	7368	1.87	9259	2.63	6583
5)		500	2.27	7627	1.83	9461	2.57	6737
6)	HT(II)	200	2.06	8405	1.68	10306	-	-
7)	HT(III)	200	2.06	8405	1.56	11100	-	-
8) FIRMEX			2.39	7244	1.99	8701	2.99	5791
9) ABRASALOY			2.48	6981	1.95	8879	2.89	5991
10) ASTRALLOY			2.40	7214	2.06	8405	2.92	5929
11) AISI 1020HR			3.02	5733	2.55	6709	3.45	5019
12) Fe/3Cr/2Mn/.5Mo/.3C Air Melt		200	2.22	7800	1.73	10008		
13) Fe/4Cr/2Mn/.3C Vac Melt		200	1.78	9727	1.49	11620		
14) Fe/4Cr/2Mn/.3C Air Melt		200	2.12	8167	-	-		
15) AISI 4340			1.58	10958	1.29	13422		
16) ATLANTIC 33			1.89	9161				
17) JR AR-Q			2.00	8657				
18) JR AR-360			2.40	7214				

*(mm/mm^3)

FIGURE CAPTIONS

Fig. 1. Illustration of heat treatments employed in this study.

Fig. 2. Sketch of wear specimen preparation from heat treated steel blank.

Fig. 3. Optical micrographs of experimental steel: (a), (b), and (c) are from HT(I), (II), and (III), respectively.

Fig. 4. Optical micrographs of commercial alloys (a) Firmex, (b) Abrasaloy, (c) Astralloy and (d) AISI 1020.

Fig. 5. TEM micrographs of experimental alloys (a) HT(I), (b) HT (III).

Fig. 6. Bright field (a) and dark field (b) micrographs showing retained austenite phase in experimental alloy following HT(II) in the 200°C tempered condition.

Fig. 7. Bright field (a) and dark field (b) of 300°C tempered experimental alloy. Note extensive twin carbide precipitation (courtesy of M. Sarikaya).

Fig. 8. Wear resistance and mechanical properties versus tempering temperature showing that tempering martensite embrittlement (occurring at ∿300°C) leads to an abrupt drop in wear resistance.

Fig. 9. Wear resistance of experimental steel run on three different abrasives showing similar tempering responses.

Fig. 10. Wear resistance as a function of ultimate tensile strength showing an increasing trend of wear resistance with increasing strength for all alloys tested. (Note: All alloys are assigned by numbers as referred to in Table 3).

Fig. 11. Wear resistance versus hardness showing a good correlation.

Fig. 12. Wear resistance showing a poor correlation to Charpy impact toughness.

Fig. 13. Positive trend exits between abrasive wear resistance and yield strength of most of the materials tested.

Fig. 14. Three types of abrasives; (a) SiC (c) Al_2O_3 (e) SiO_2 before the wear tests and (b) SiC (d) Al_2O_3 (f) SiO_2 after the wear tests.

Fig. 15. General wear surfaces of (a) Quatough steel tempered at 200°C (b) AISI 1020 (c) Quatough steel tempered at 500°C (d) Abrasaloy (e) Firmex and (f) Astralloy. Abrasives used in the wear tests are 120 grit SiC.

Fig. 16. General wear surface of Quatough steel (as quench) was abraded by 120 grit SiC. Embedded abrasive particles are observed.

Fig. 17. SEM micrographs show the difference between the appearences of surfaces under different abrasives.

(a) Quatough steel (as quench) abraded by 120 grit SiC.

(b) Same material abraded by 40 grit SiO_2.

(c) AISI 1020 abraded by 120 grit SiC.

(d) AISI 1020 abraded by 40 grit SiO_2.

Fig. 18. SEM micrographs show the microcutting as material is sheared off by abrasives. EDX picture (c) is taken from area (A) in micrograph (b). EDX picture (d) is taken from area (c) which show a large amount of silicon present and this may indicate SiC abrasive is embedded at the wedge (B).

Fig. 19. Microgarphs show 2 cracks join at area (B). The formation of debris is due to delamination.

Fig. 20. (a) AISI 1020 wear debris from wear test using 120 grit SiC.

(b) X-ray map of Fe show the profile of wear debris.

(c) X-ray map of Si.

Fig. 21. Bar graph showing comparison of different allow worn by 120 grit SiC.

Fig. 22. Bar graph showing comparison of different alloys worn by 120 grit Al_2O_3.

Fig. 23. Bar graph showing comparison of different alloys worn by 40 grit SiO_2.

HEAT TREATMENTS

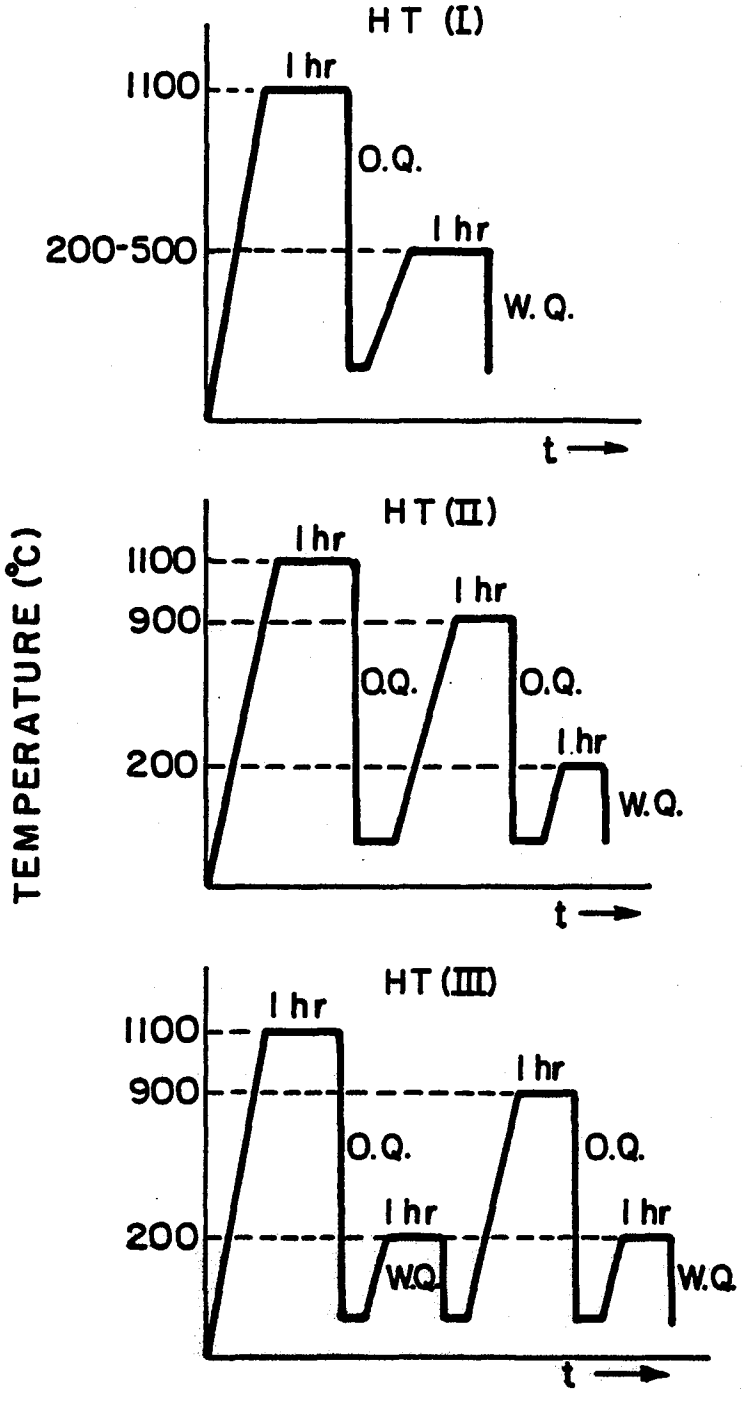

XBL 819-6556

Fig. 1

WEAR SPECIMEN PREPARATION

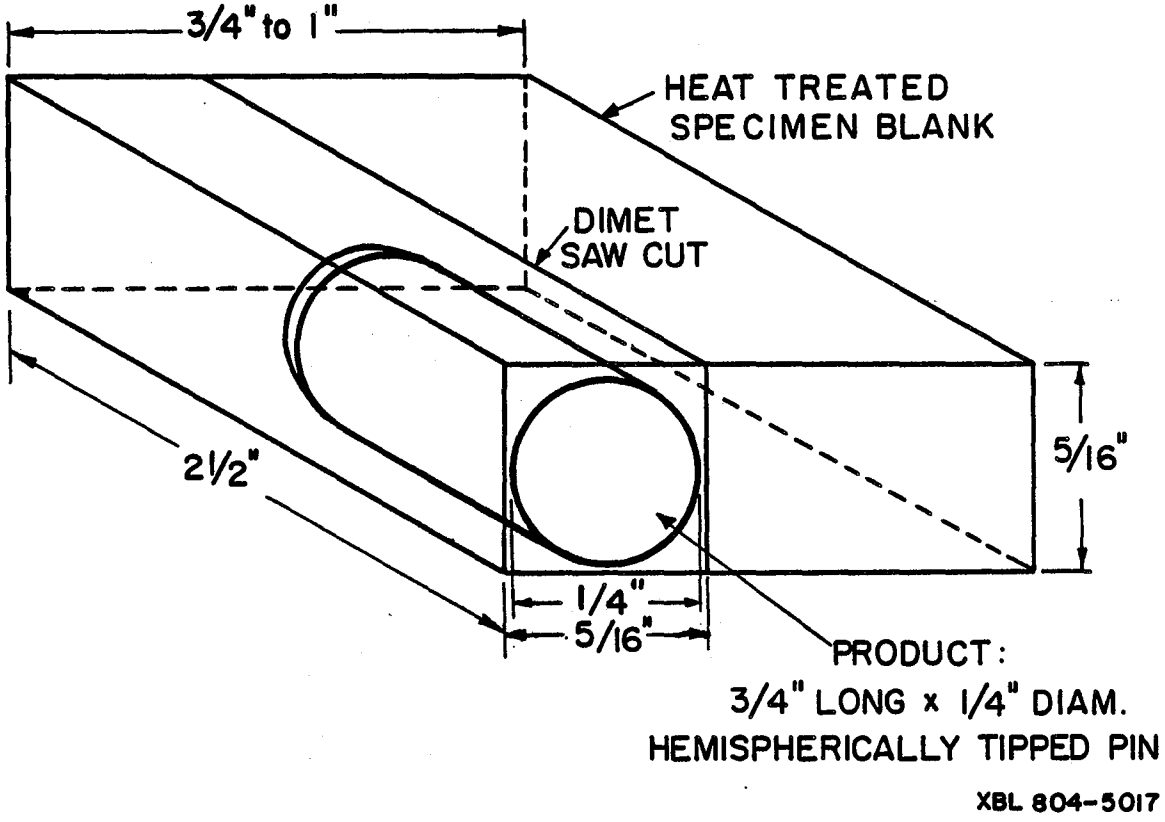

Fig. 2

XBB 810-9825

Fig. 3

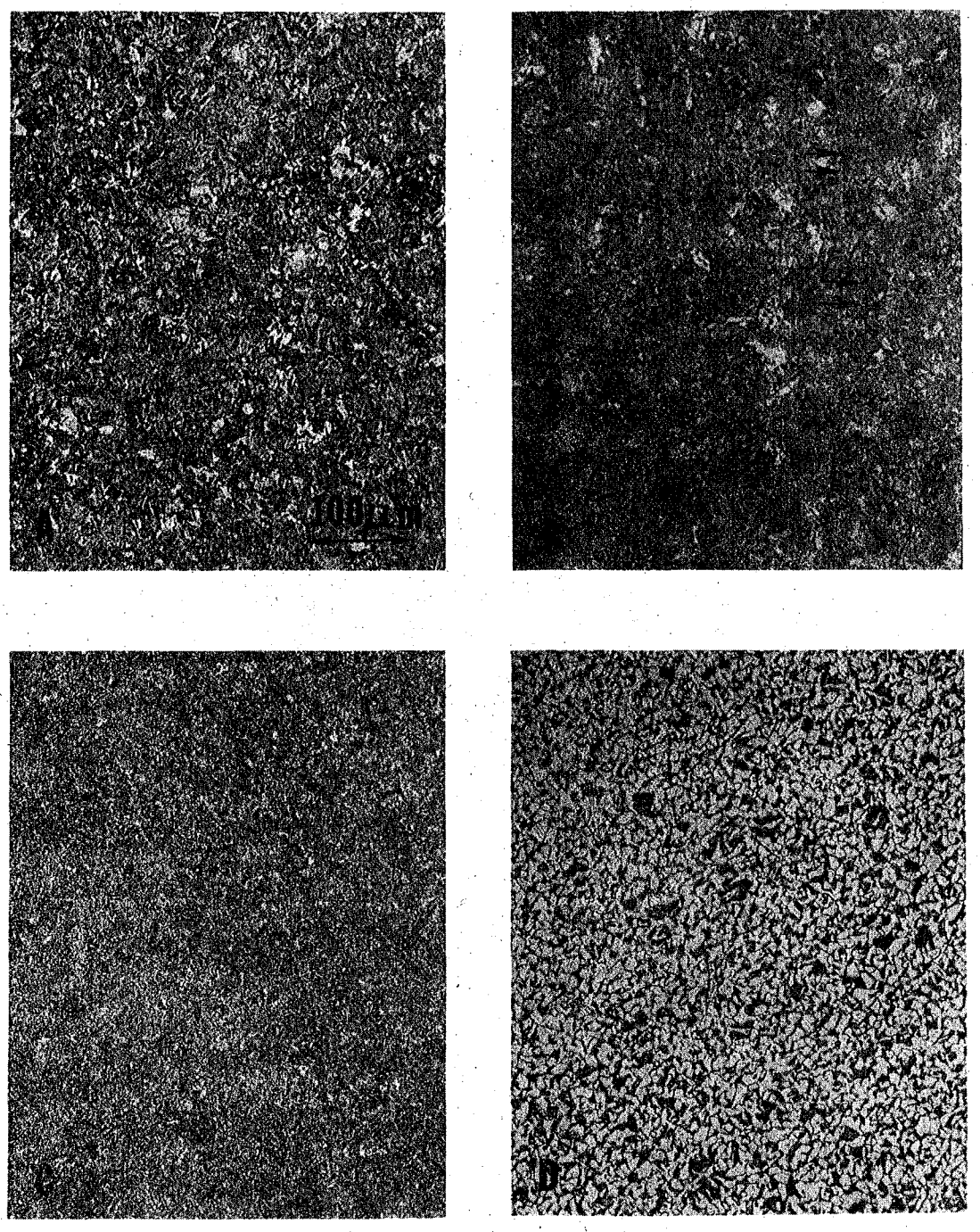

XBB 810-9832

Fig. 4

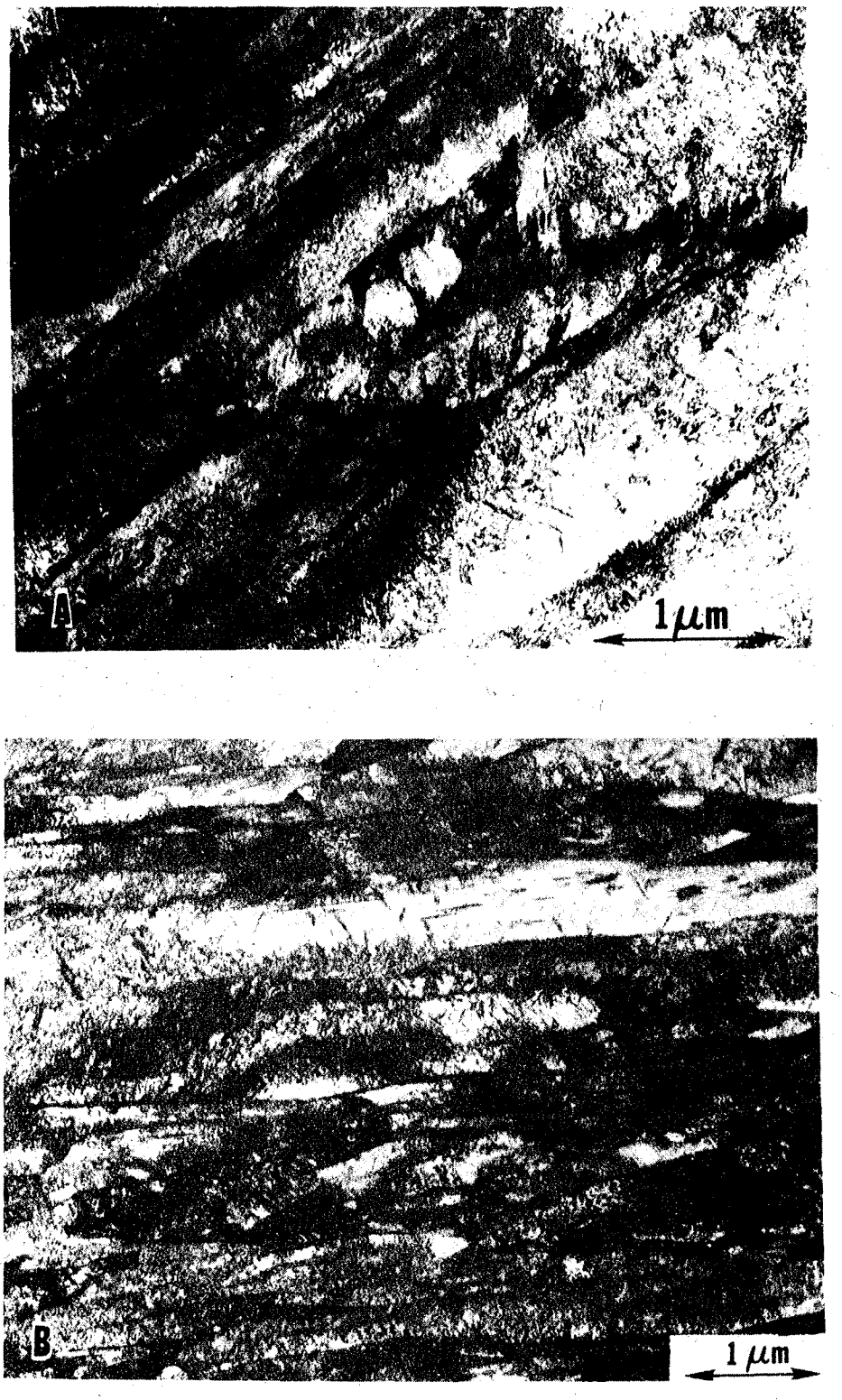

Fig. 5 XBB 810-11084

Fig. 6

XBB 810-9831

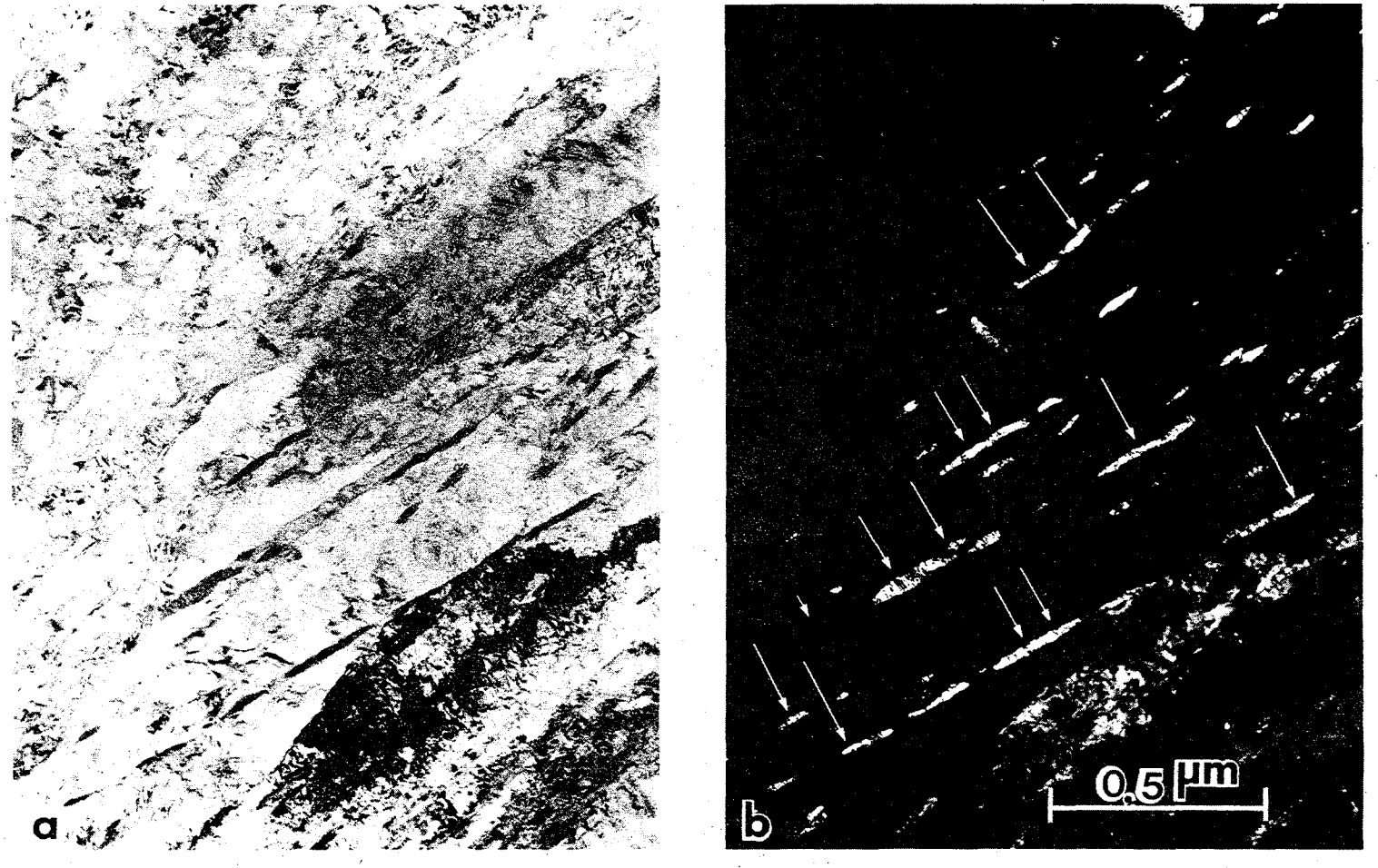

Fig. 7

XBB 794-5669

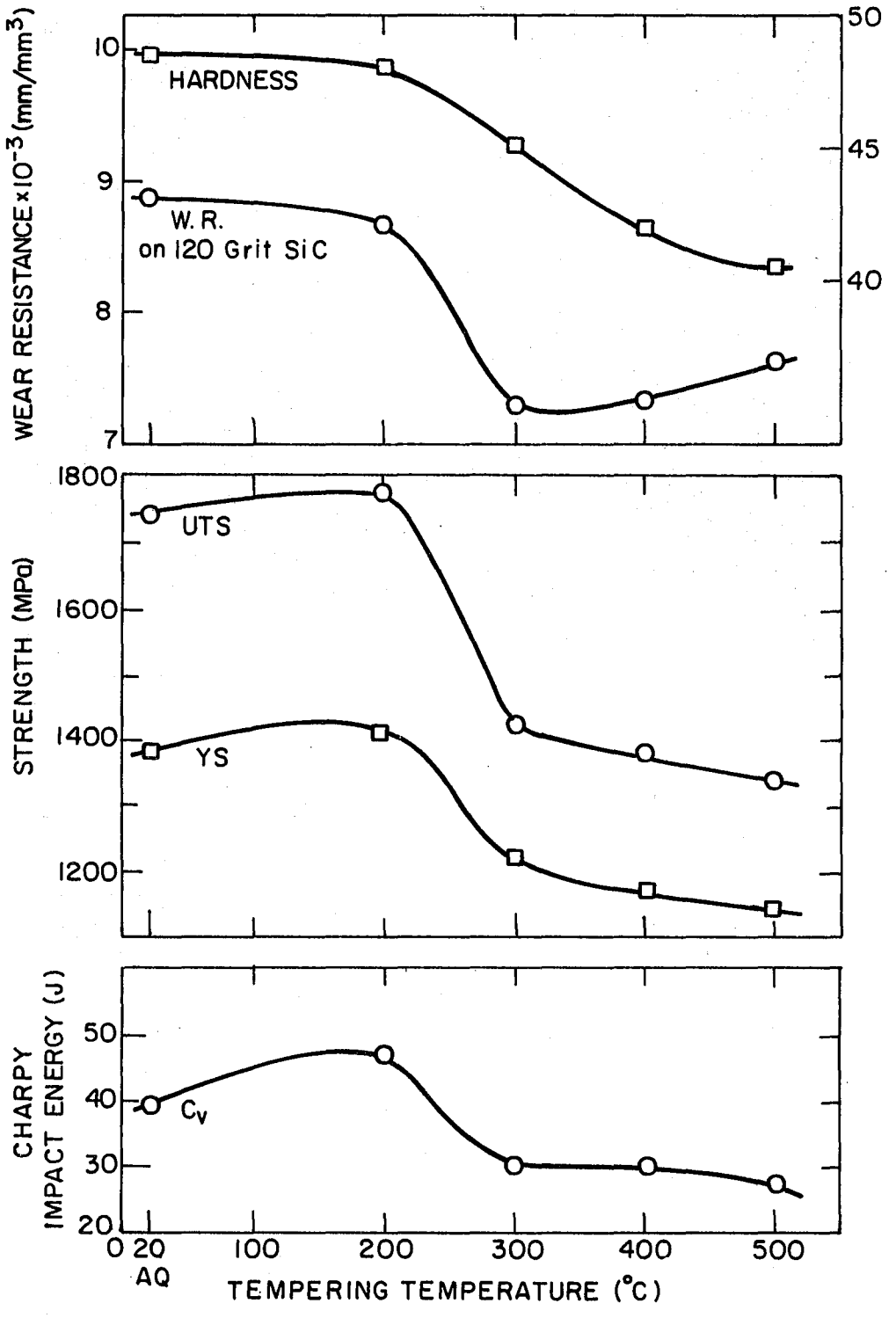

XBL 819-6555

Fig. 8

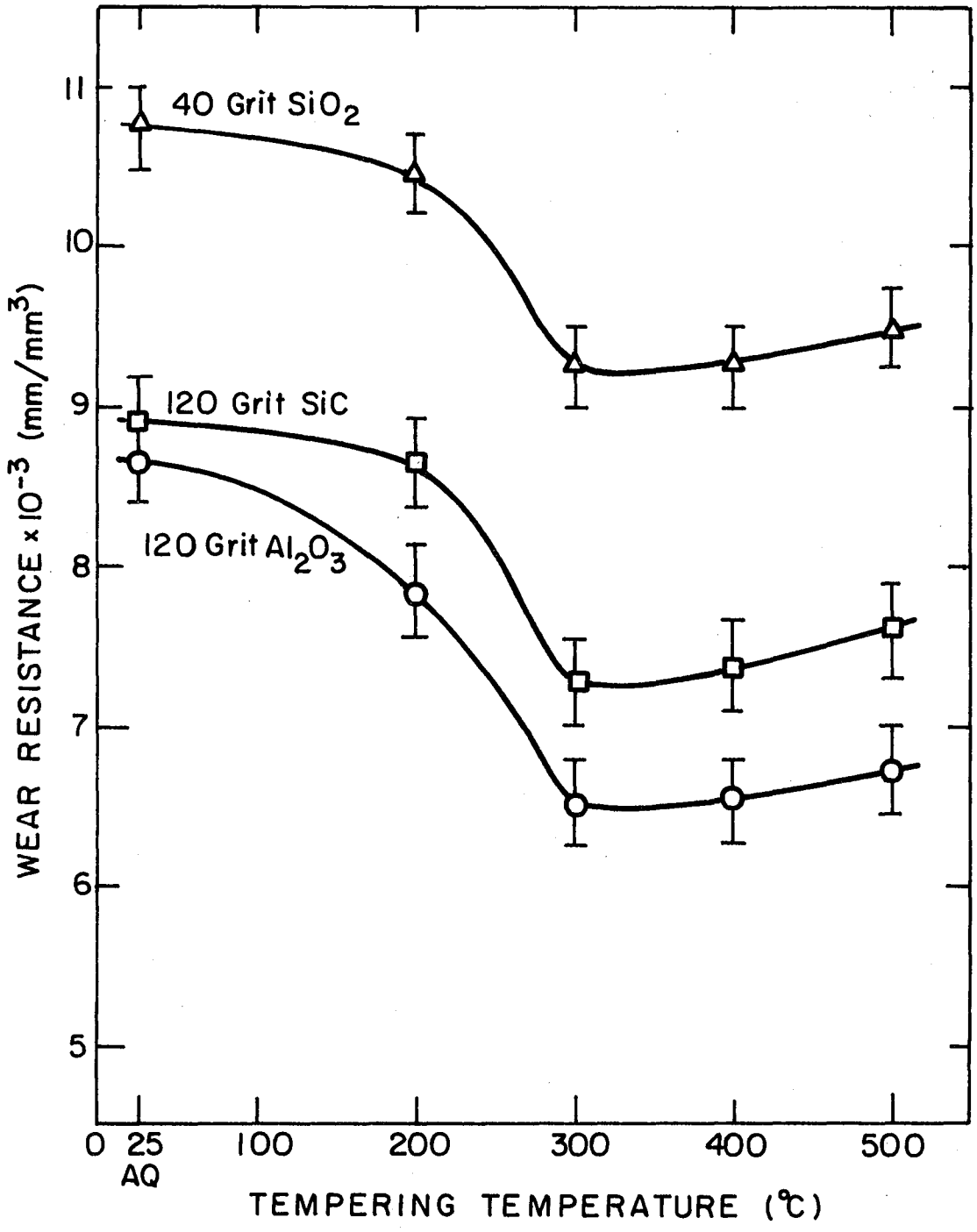

XBL 819-6554

Fig. 9

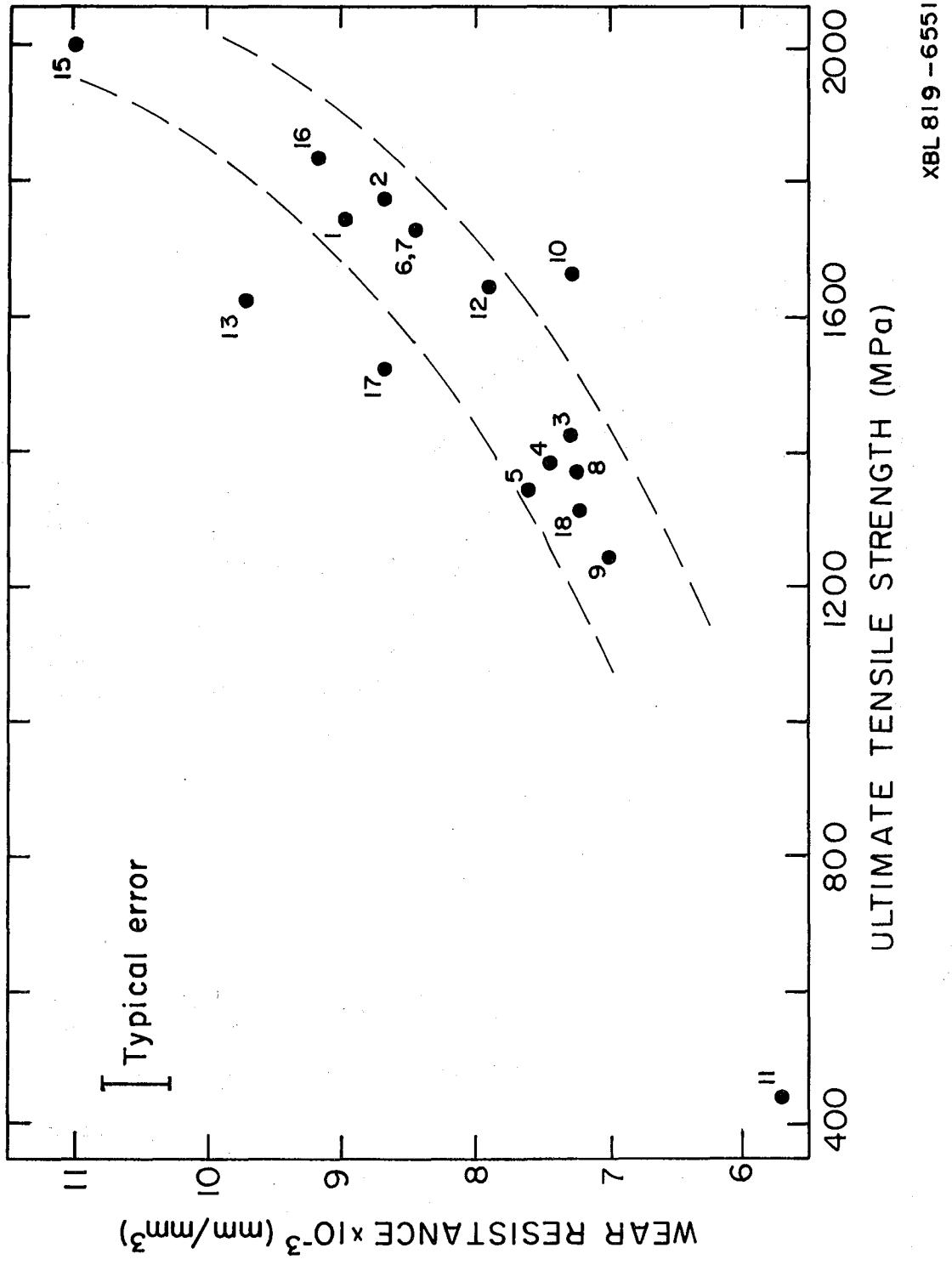

XBL 819-6551

Fig. 10

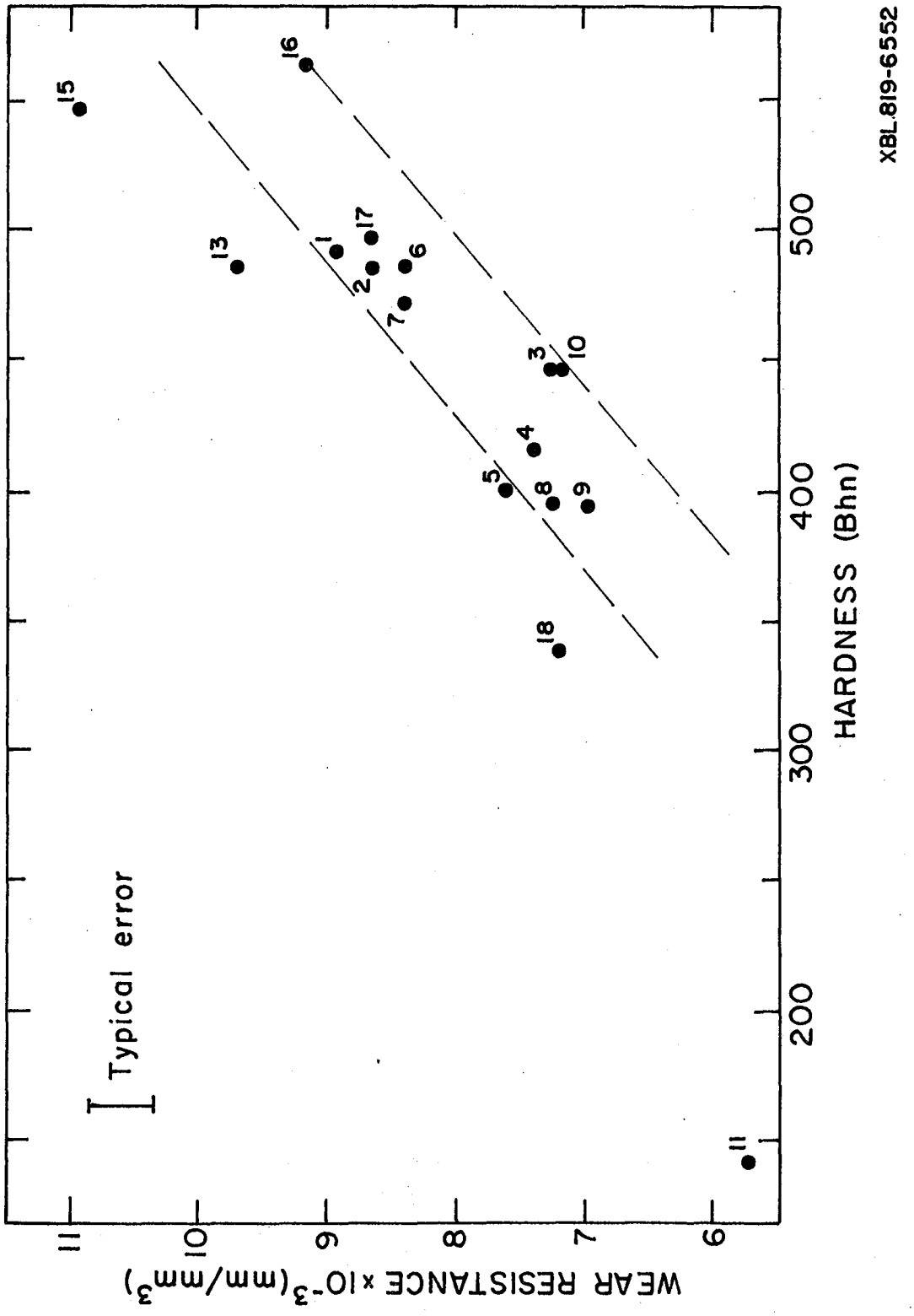
WEAR RESISTANCE × 10⁻³ (mm/mm³)
11
10
9
8
7
6
HARDNESS (Bhn)
200
300
400
500
Typical error
1
2
3
4
5
6
7
8
9
10
11
13
15
16
17
18
XBL 819-6552

Fig. 11

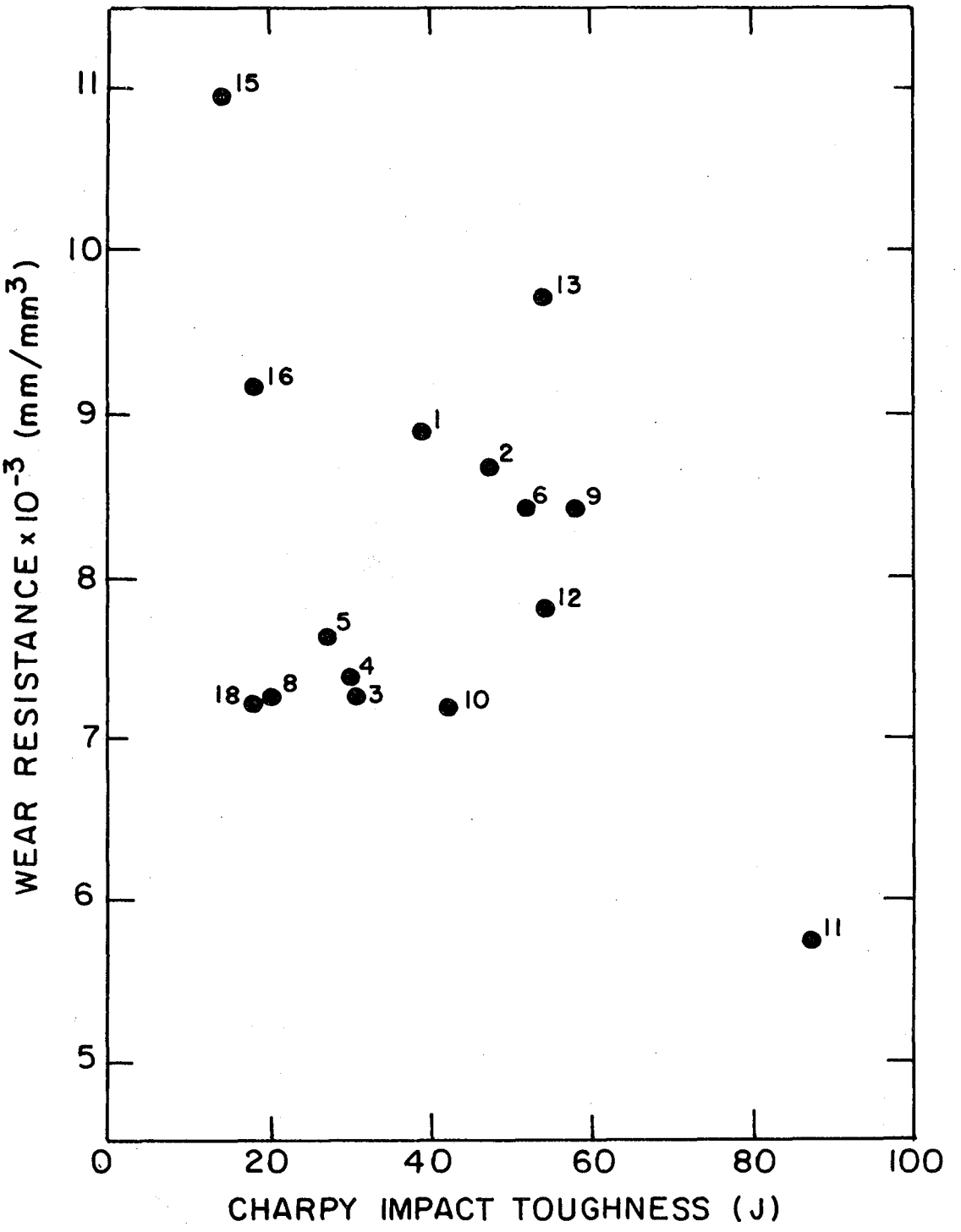

XBL 819-6553

Fig. 12

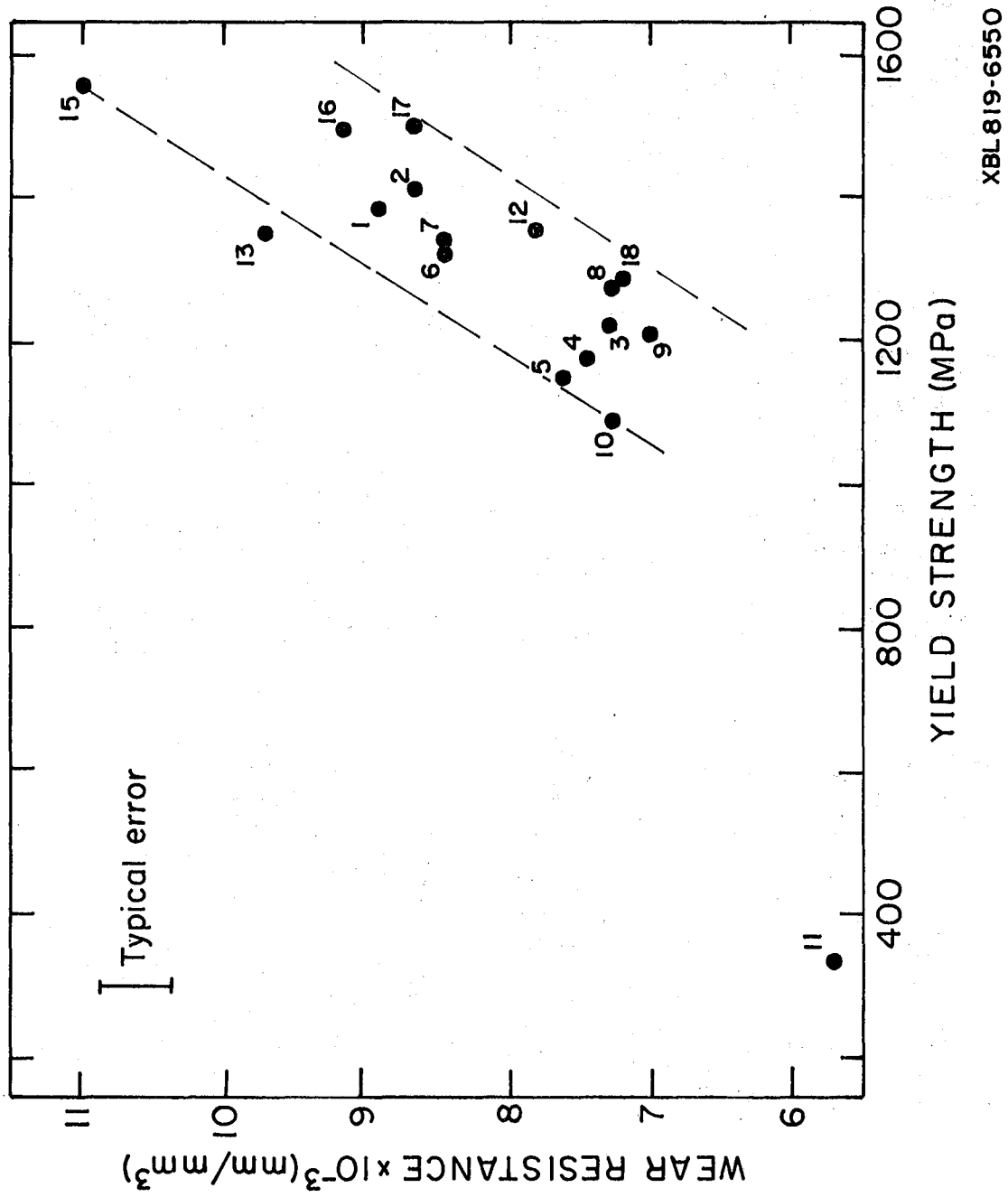
WEAR RESISTANCE x10⁻³(mm/mm³)
11
10
9
8
7
6
YIELD STRENGTH (MPa)
400
800
1200
1600
Typical error
1
2
3
4
5
6
7
8
9
10
11
12
13
15
16
17
18
XBL 819-6550

Fig. 13

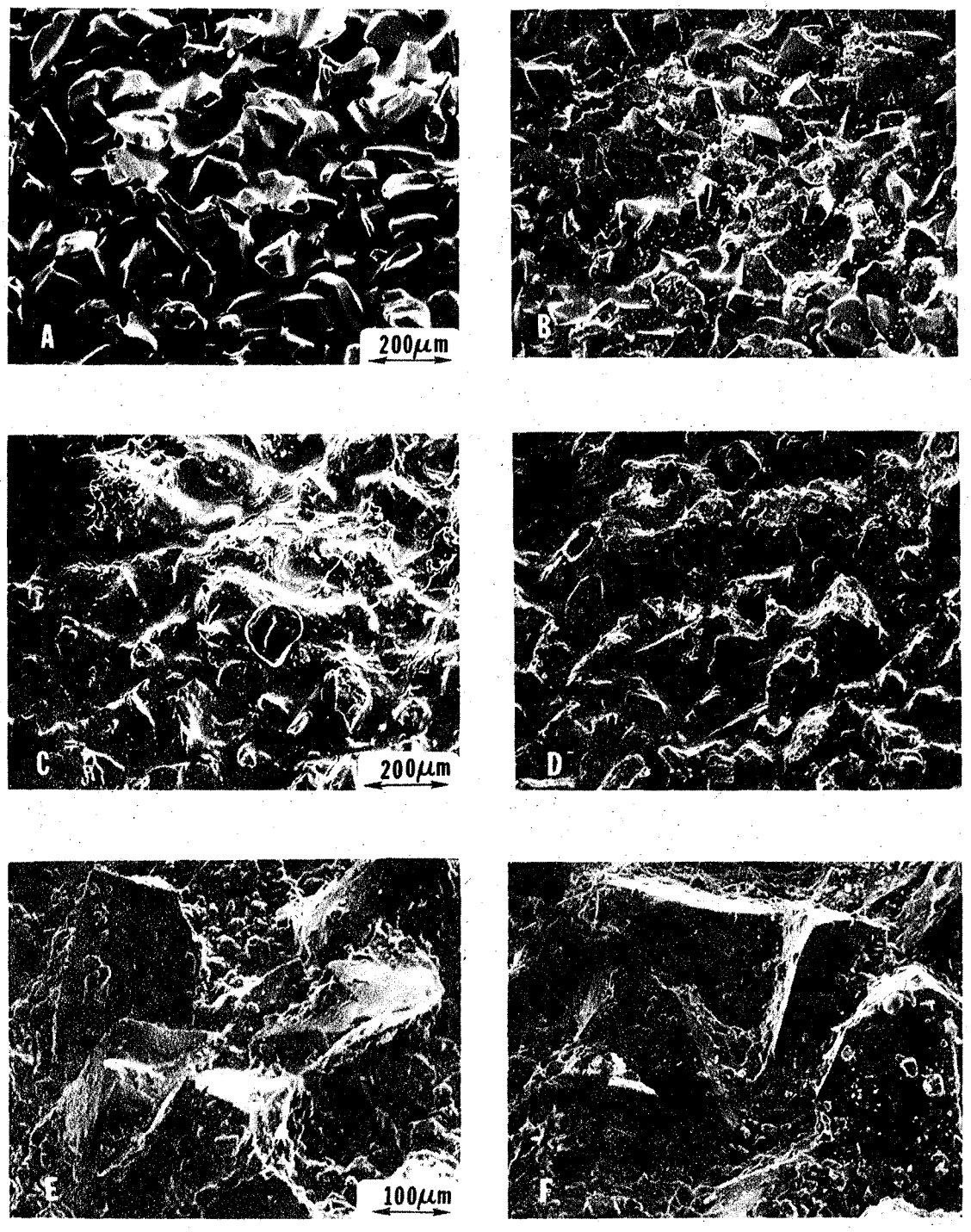

Fig. 14 XBB 810-9824

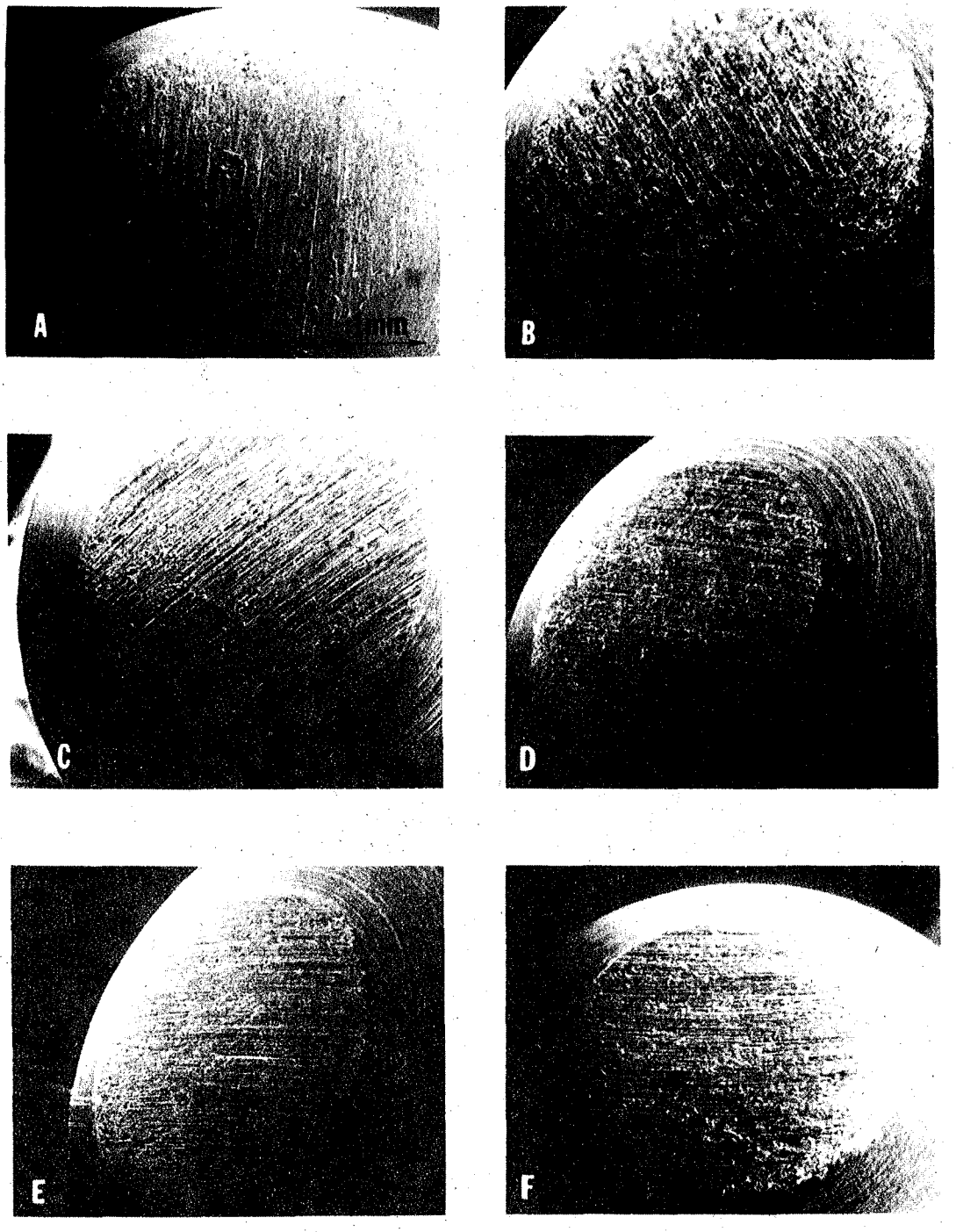

XBB 810-9829

Fig. 15

Fig. 16 XBB 810-9828

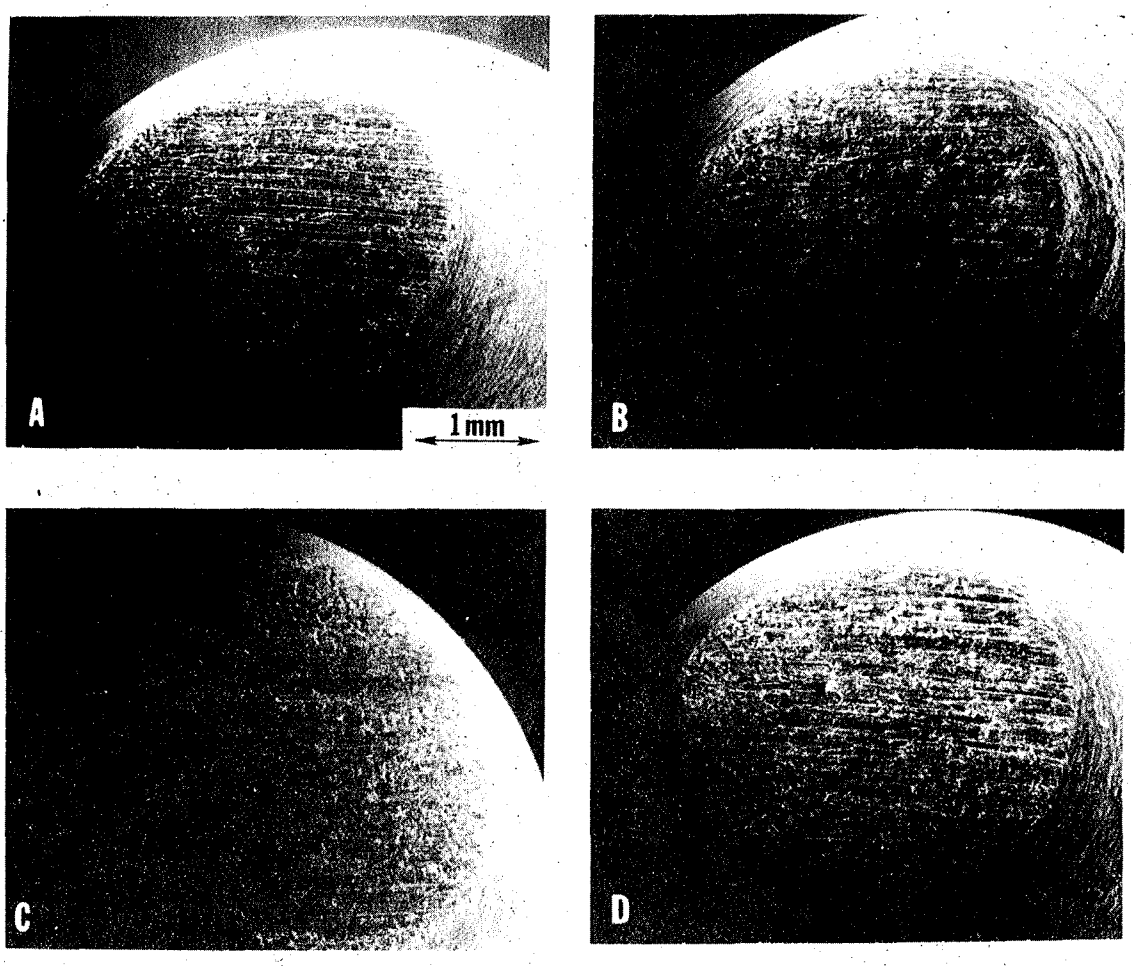

XBB 810-9877

Fig. 17

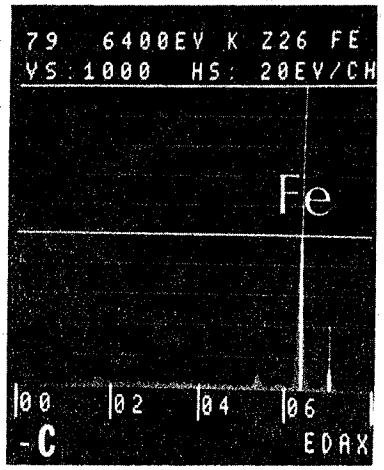

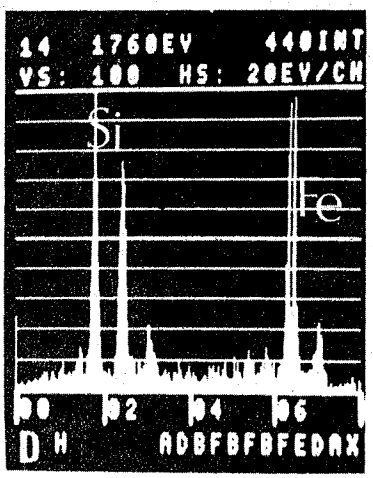

Fig. 18

XBB 810-9830

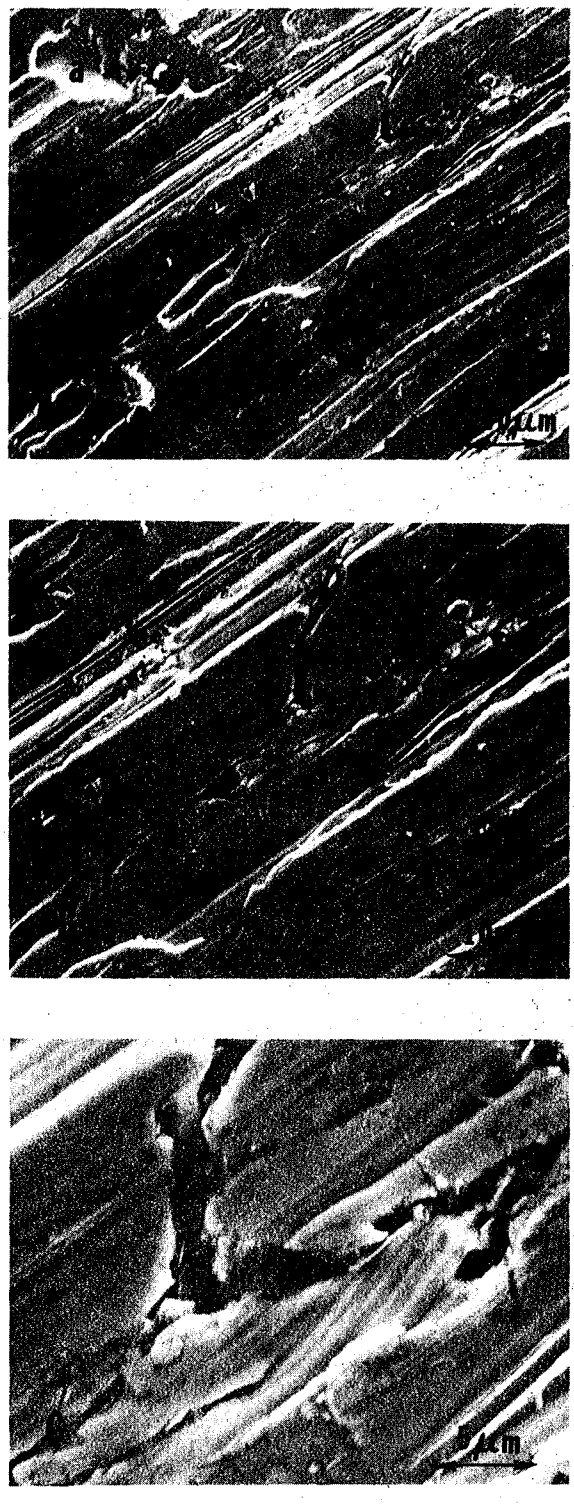

XBB 810-9826

Fig. 19

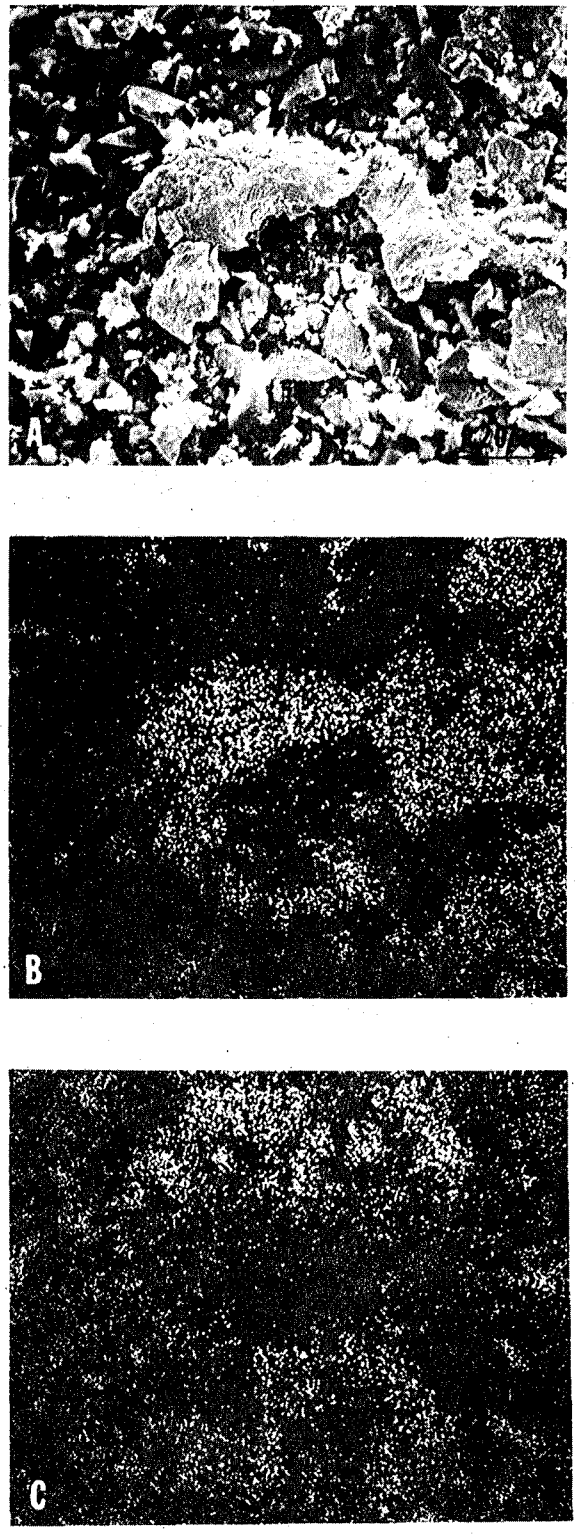

XBB 810-9827

Fig. 20

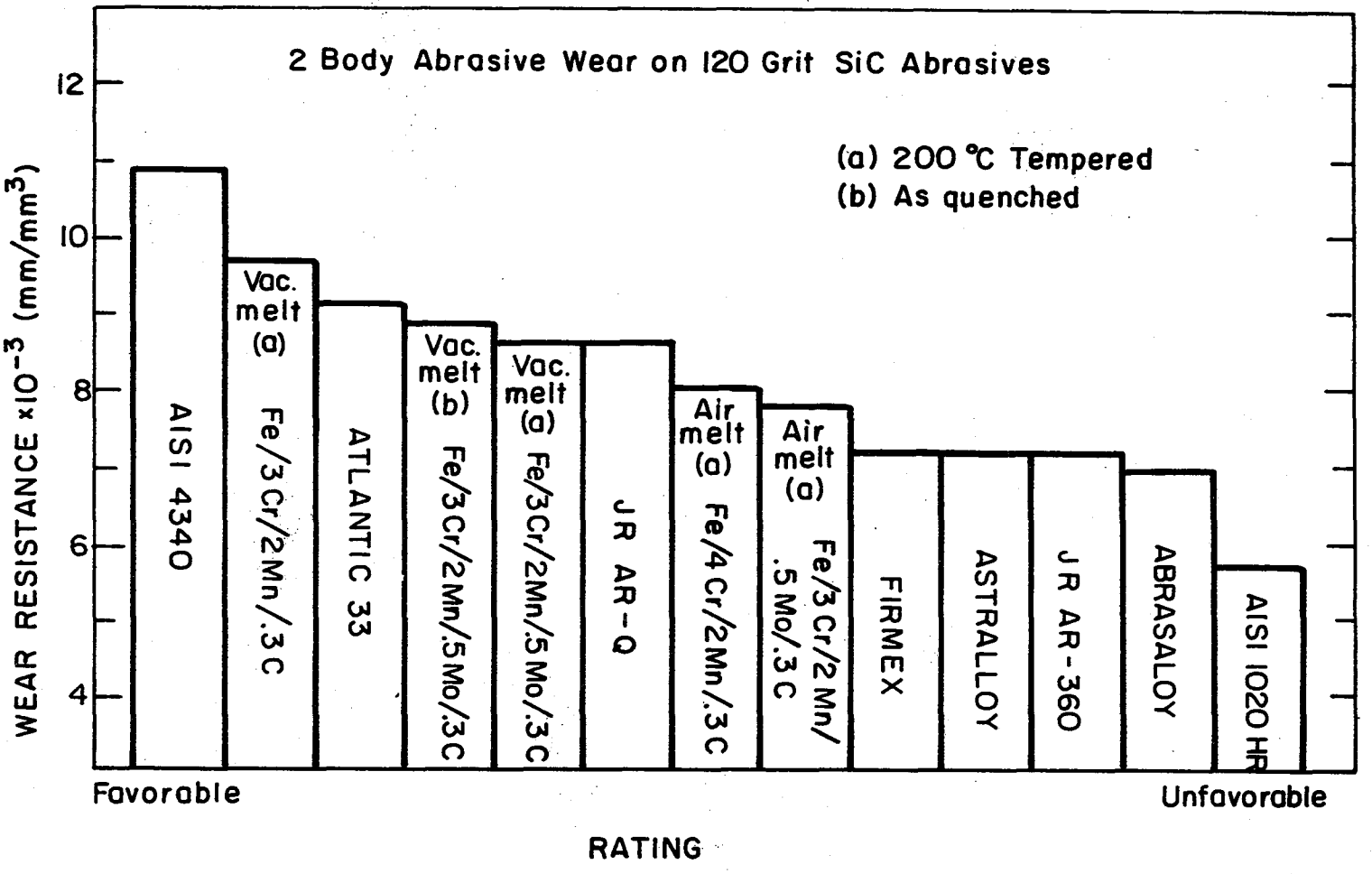

XBL 819-6558

Fig. 21

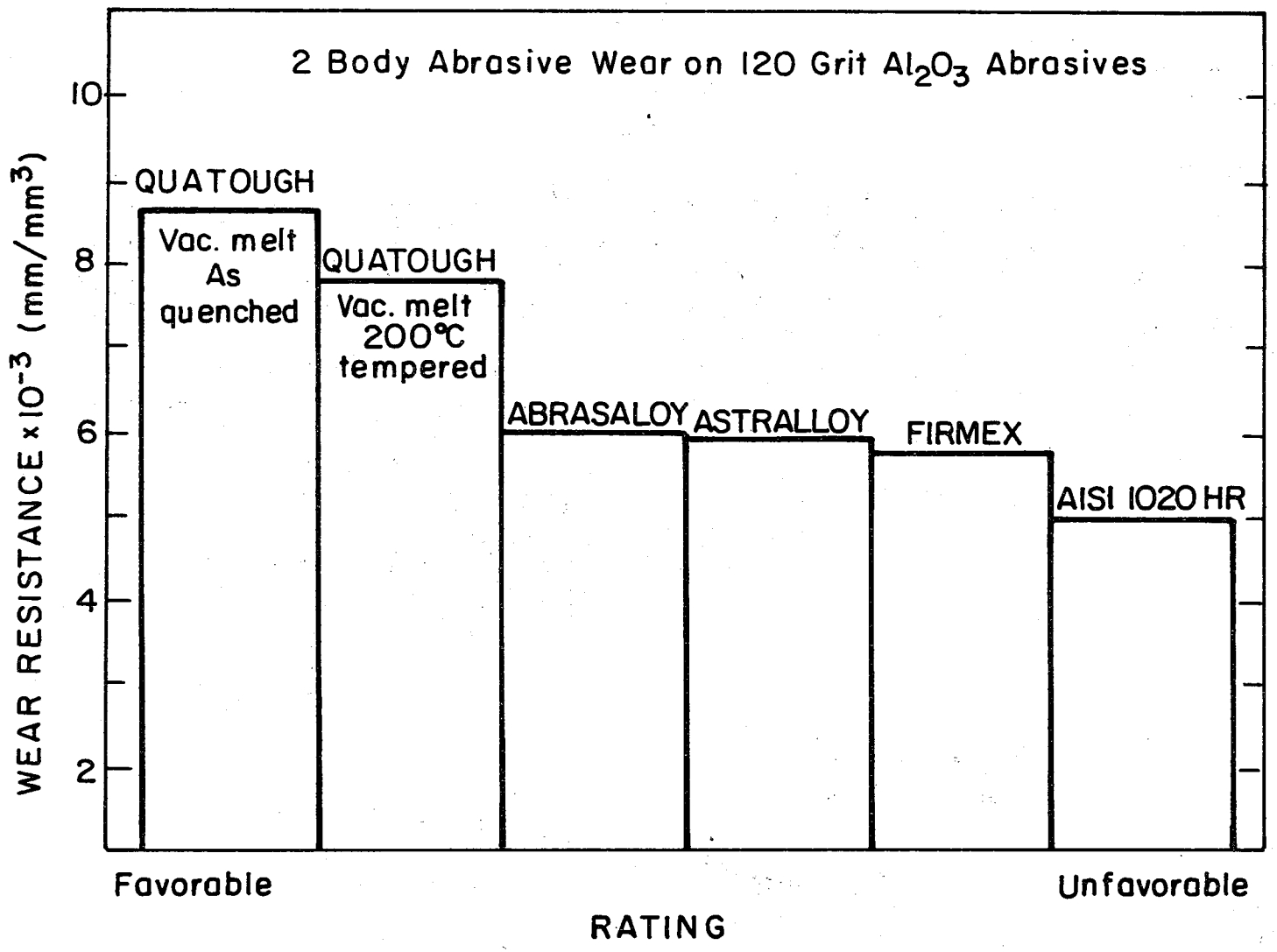
2 Body Abrasive Wear on 120 Grit Al_2O_3 Abrasives
WEAR RESISTANCE x 10^{-3} (mm/mm^3)
10
8
6
4
2
QUATOUGH
Vac. melt
As
quenched
QUATOUGH
Vac. melt
200°C
tempered
ABRASALOY
ASTRALLOY
FIRMEX
AISI 1020 HR
Favorable
Unfavorable
RATING
XBL 819-6559

Fig. 22

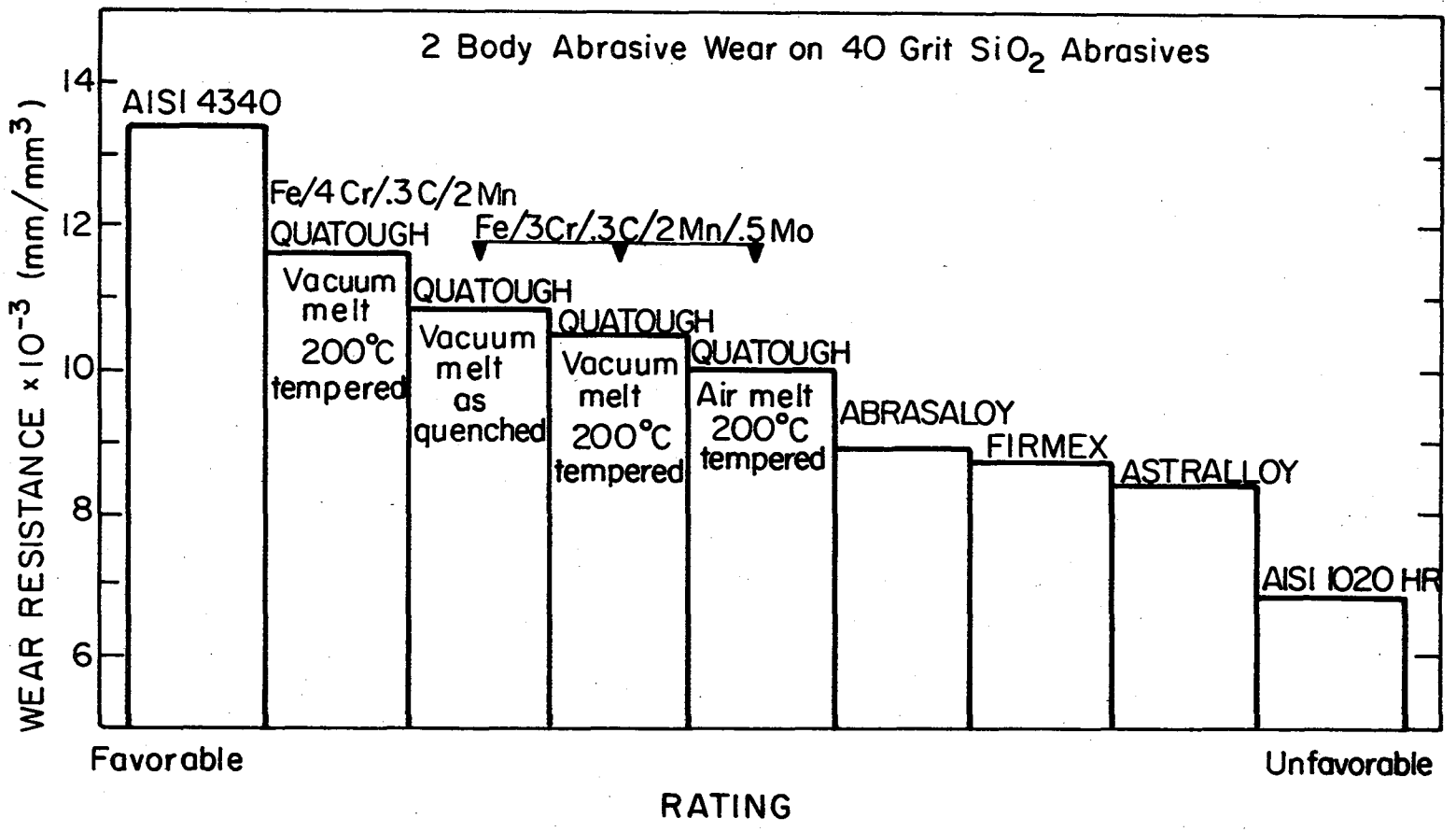

XBL 819-6557

Fig. 23